



**REPUBLIC OF IRAQ
MINISTRY OF HIGHER EDUCATION AND SCIENTIFIC
RESEARCH**

**AL-FURAT AL-AWSAT TECHNICAL UNIVERSITY
ENGINEERING TECHNICAL COLLEGE - NAJAF**

**EXPERIMENTAL AND NUMERICAL
SIMULATION OF A DUAL-PURPOSE
SOLAR THERMAL COLLECTOR**

A THESIS

**SUBMITTED TO THE POWER TECHNICAL ENGINEERING
DEPARTMENT IN PARTIAL FULFILMENT OF THE
REQUIREMENTS FOR THE DEGREE OF TECHNICAL MASTER
IN MECHANICAL ENGINEERING –THERMAL**

BY

JAFER SHANDAL MUTAR

(B.SC AUTOMOBILE ENGINEERING 2013)

Supervisor by

Asst. prof. Dr. QAHTAN ADNAN ABED

September 2020

بِسْمِ اللَّهِ الرَّحْمَنِ الرَّحِيمِ

رَبِّ أَوْزَعْنِي أَنْ أَشْكُرَ نِعْمَتَكَ الَّتِي أَنْعَمْتَ عَلَيَّ
وَعَلَىٰ وَالِدَيَّ وَأَنْ أَعْمَلَ صَالِحًا تَرْضَاهُ وَأَصْلِحْ لِي
فِي ذُرِّيَّتِي ۖ إِنَّيٓ أَخَوٰهُنَّ الْمُسْلِمِينَ

صَدَقَ اللَّهُ الْعَلِيُّ الْعَظِيمُ

....

سورة الأحقاف: آية ١٥

الإهداء

إلى رفيق دموع المظلومين والمنتظرين... الأمل حيث تبدد الأمل... صاحب
العصر والزمان

إلى الوطن الذي تلقى بصدرة سهام الزمن لإكمال صلاة العمر بسلام... إليه حيث
روحه... الفقيد والدي

إلى السومرية السمراء التي يتدفق تنورها الطيني بلظى قلبها... المجاهدة
والمثكولة... والدتي العظيمة

إلى سلالة السبعين المُخْلِصَة... إلى الضاحكين بوجه المنايا استصغاراً لها...
إخوتي الشهداء... محمد وأحمد

إلى صنو القلب وقسيم الروح... إلى العزم الذي أطلبه دمعاً... الصديق والأخ...
الشهيد أحمد ساجت

إلى عثاكيل النور المتدليات من نحر الحسين ... شهداء الوطن جميعاً

إلى المرابي الفاضل والملهم المعطاء... الصديق والشيخ الفقيد ستار الصفرائي

إلى بقية الجرح والسند العتيد... إخوتي وأصدقائي.

إلى شريكة الدرب ومقتسمة الألم ... زوجتي الصبور

أهدي عملي هذا...

DISCLAIMER

I confirm that the work submitted in this thesis is my own work and has not been submitted to another organization or for any other degree.

Jafer Shandal Mutar

Signature:

Date

ACKNOWLEDGMENT

Before every one and above all estimators my thinking, praise and gratitude goes to ALLAH almighty. Who provided all that was needed to complete this research. My sincerest gratitude goes to the pure dynasty of Mohammad and his family. Secondly, my deepest grateful goes to Asst. Prof. Dr. Qahtan A. Abed the man who is doing with his knowledge. My words cannot express my thankfulness to him. My appreciation also goes to the head of department Asst. Prof. Dr. Dhafer Manea Hachim who helped me during my work. I am also grateful to all my teachers throughout my academic career who they provided me with motivations and encouragement. My appreciation goes to my brothers and friends who stood with me in weal and woe. Lastly, all the respect and love goes to the spirit of my father. The deceased who accompany me with his litany as well as the benediction of my greet mother and my brothers martyrs and dear my wife. At the same time my sincerest gratitude goes to everyone who helped me to accomplish this humble research.


JAFER SHANDAL MUTAR

(B.SC AUTOMOBILE ENGINEERING)

September 2020

Supervisor Certification

We certify that this thesis titled” **Experimental And Numerical Simulation Of A Dual-Purpose Solar Thermal Collector**” which is being submitted by **Jafer Shandal Mutar** was prepared under our supervision at the Power Techniques Engineering Department, Engineering Technical faculty-Najaf, AL- Furat Al-Awsat Technical University, as partial fulfillment of the requirements for the degree of Master of technical in thermal Engineering.

Signature: 

Name **Asst. Prof. Dr. Qahtan Adnan Abed**

(Supervisor)

Date 20/12/2020

In view of the available recommendation, we forward this thesis for debate by the examining committee.

Signature:

Name: **Assist. Prof. Dr. Dhafer Manea Hachim**

(Head of power Tec.Eng.Dept.)

Date: / / 2020


Committee Report

We certify that we have read this thesis titled” **Experimental And Numerical Simulation Of A Dual-Purpose Solar Thermal Collector**” which is being submitted by **Jafer Shandal Mutar** and as Examining Committee, examined the student in it is contents. In our opinion, the thesis is adequate for an award of degree of Master of Technical in Thermal Engineering.

Signature: 

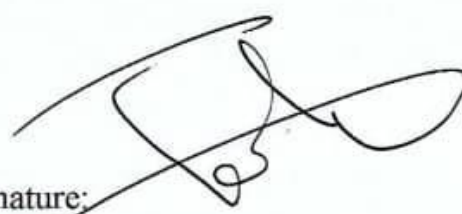
Name: **Asst. Prof. Dr. Qahtan Adnan Abed**
(Supervisor)

Date 20 / 12 / 2020

Signature: 


Name: **Asst. Prof. Dr. Mahdi H. Kadhum**
(Member)

Date / / 2020

Signature: 

Name: **Asst. Prof. Dr. Tahsean A. Hussain**
(Member)

Date / / 2020

Signature: 

Name: **Prof. Dr. Nabil J. Yasin**
(Chairman)

Date 7 / 12 / 2020

Approval of the Engineering Technical College – Najaf.

Signature:

Name: **Asst. prof. Dr. Hassanain Ghani Hameed**
Dean of Technical Engineering College -Najaf

Date: / / 2020

ABSTRACT

In this research, study the performance of dual purpose solar thermal collector experimentally and numerically simulation was done. The study include using a new type of absorber plate and water pipes distribution. The simulation part of this research is done by using COMSOL Multiphysics program version 5.5. The new type was corrugated absorber plate with (2*1) m dimensions and zig-zag water pipes with (0.01) m diameter passage through the absorber plate.

The experimental work is done in Al-Muthanna city, Iraq with latitude 31°N and longitude 45° E. The effect of solar irradiance, ambient temperature, wind speed, water volumetric flow and inlet water temperature on the performance of the dual purpose solar thermal collector was studied. The numerical simulation concludes that the present work achieved enhancement in efficiency of collector by 2.4% comparison with previous study, and also that when the solar irradiance, inlet water temperature and ambient temperature increases the outlet temperature increases, but it decreases with the wind speed and volumetric flow increases. There was a good agreement between the numerical simulation and experimental results with average error about 4.72%.

The experimental work included studying the effect of the three values of volumetric flow (40, 60 and 80) L/h in June and July, 2020. The experimental results show that the optimum rate of volumetric flow is 40 L/h. the maximum outlet temperature for water and air was (69.9 and 79.2) °C respectively. The maximum values of efficiency recorded was (83.3, 80.4 and 78.5) % for flow rate of (40, 60 and 80) L/h respectively.

CONTENTS

DISCLAIMER.....	I
ACKNOWLEDGMENT	II
Supervisor Certification	III
Committee Report	IV
ABSTRACT	V
CONTENTS	VI
LIST OF TABLES	IX
LIST OF FIGURES.....	X
NOMENCLATURE.....	XIII
DIMENSIONLESS GROUP.....	XIV
CHAPTER ONE	1
INTRODUCTION.....	1
1.1 Renewable energy	1
1.1.1 Advantage of renewable energy	1
1.1.2 Disadvantage of renewable energy	2
1.1.3 Types of renewable energy	2
1.2 Solar energy.....	2
1.3 Solar thermal collector	4
1.3.1 Flat plate solar collector (FPSC)	6
1.3.2 Components of dual purpose solar collector.....	6
1.3.3 Application of dual purpose solar collector	7
1.4 Research objectives	8
CHAPTER TWO	9
LITERATURE REVIEW.....	9
2.1 Introduction	9
2.2 Studies about the solar air collectors.....	9
2.3 Studies about the solar water collectors	14

2.4 Studies about the dual-purpose solar collectors	17
2.5 Summary	21
CHAPTER THREE	28
NUMERICAL SIMULATION	28
3.1 Comsol introduction	28
3.2 Building of model.....	29
3.3 Properties of the material used	30
3.4 Physics of study	32
3.5 Mesh generation	32
3.6 Steps of numerical solution	33
3.7 Assumption of model	35
3.8 Mathematical of dual purpose solar collector (DPSC)	35
3.8.1 Covering equations.....	35
3.8.2 Boundary condition	36
CHAPTER FOUR	37
EXPERIMENTAL WORK	37
4.1 Introduction	37
4.2 Experimental rig	37
4.2.1 Dual purpose solar collector.....	38
4.2.2 Water pump	42
4.2.3 Fan.....	42
4.3 The measurement devices	43
4.3.1 Data loggers.....	43
4.3.2 Temperature sensors.....	44
4.3.3 Solar power meter	45
4.3.4 Anemometer	46
4.3.5 Water flow meter.....	47
CHAPTER FIVE	48
RESULTS AND DISCUSSION	48
5.1 Introduction	48

5.2 Numerical simulation results.....	48
5.2.1 Validation of model.....	48
5.2.2 Effect of ambient temperature.....	49
5.2.3 Effect of solar irradiance	51
5.2.4 Effect of outlet air velocity.....	52
5.2.5 Effect of inlet water temperature.....	53
5.2.6 Effect of water volume flow rate.....	54
5.2.7 Results of winter simulation days	55
5.2.8 Temperature distribution study	58
5.3 Experimental results	61
5.3.1 Comparison between experimental and numerical results of present work	61
5.3.2 The effect of weather condition	64
5.3.3 Temperature differences results	70
5.3.4 The efficiency of collector	71
CHAPTER SIX	74
CONCLUSION AND RECOMMENDATIONS	74
6.1 The conclusion	74
6.2 The recommendations	75
Appendix (A).....	A-1
The calibration of Instruments used in the experiments	A-1
A.1 Calibration of solar collector meter:.....	A-1
A.2 Flow rate meter calibrate method.....	8-A
A.3 Calibration of temperature sensors of 8- channel data logger and 4K type thermocouples with digital thermometers:.....	A-3
Appendix (B).....	B-1
The experimental results	B-1
Appendix (C).....	C-1
Uncurtains analysis.....	C-1
Appendix (D).....	D-1
List of publications.....	D-1

LIST OF TABLES

Table No.	Title of the Tables	Page No.
Table 2-1	Literature review summary.....	21
Table 3-1	Description, symbol and dimensional of model.	29
Table 4-1	Specifications of dual purpose flat plate solar collector.....	42
Table 4-2	The specification of the water pump.	42
Table 4-3	The specification of fan.	43
Table A.1	Calibration results of first 8- channels data logger with 8 sensors...A-3	
Table A.2	Calibration results of second 8-channels data logger with 8 sensors.A-4	
Table A.3	The calibration of 4 k- type thermocouple.....A-5	
Table B-1	Experimental results.....	B-1

LIST OF FIGURES

Figure No.	Title of the Figure	Page No.
Fig. 1.1:	The global solar radiation in World 2019.....	3
Fig. 1.2:	The global solar radiation in Iraq 2019.....	4
Fig. 1.3:	Solar collector types.....	5
Fig. 1.4:	Component of DPSC.	7
Fig. 2.1	Solar air collector system.....	10
Fig. 2.2:	Copper pipes arrangement inside the wood box.	15
Fig. 3.1:	Water pipe domain.....	30
Fig. 3.2:	Absorber plate domain.....	30
Fig. 3.3:	Air domain.	31
Fig. 3.4:	Glass domain.....	31
Fig. 3.5:	Mesh generation.....	32
Fig. 3.6:	Simulation methodology.....	34
Fig. 4.1:	Photo for DPSC system with measurment devices.	38
Fig. 4.2	Cross section of DPSC.....	38
Fig. 4.3:	Schametic of experimental rig.	39
Fig. 4.4:	Absorber plate.....	40
Fig. 4.5:	Casing.	41
Fig. 4.6:	Fan.....	43
Fig. 4.7:	Data logger.....	44
Fig. 4.8:	Temperature sensors.	45
Fig. 4.9:	Solar power meter.....	46
Fig. 4.10:	Anemometer.....	47
Fig. 4.11:	Water flow meter.	47
Fig. 5.1:	Comparison between experimental results of Omid [12] with numerical results of present work of efficiency.	49

Fig. 5.2: Variation of outlet temperature with ambient temperature variation. 50

Fig. 5.3: Variation of outlet temperature with variation of solar irradiance. 51

Fig. 5.4: Variation of outlet temperature with variation of outlet air velocity. 52

Fig. 5.5: Variation of outlet temperature with variation of inlet water temperature.
..... 53

Fig. 5.6: Variation of outlet temperature with variation water volume flow rate. 54

Fig. 5.7: Solar irradiance for simulation days. 55

Fig. 5.8: Wind speed for simulation days. 56

Fig. 5.9: Ambient temperature for simulation days. 56

Fig. 5.10: Outlet water temperature for simulation days. 57

Fig. 5.11: Outlet air temperature for simulation days. 58

Fig. 5.12: Temperature contour 19/6/2020. 59

Fig. 5.13: Temperature contour 2/7/2020. 60

Fig. 5.14: Comparison between experimental and numerical results of present work of outlet air temperature, (19/6/2020). 61

Fig. 5.15: Comparison between experimental and numerical results of present work of outlet water temperature, (19/6/2020). 62

Fig. 5.16: Comparison between experimental and numerical results of present work of outlet air temperature, (2/7/2020). 62

Fig. 5.17: comparison between experimental and numerical results of present work of outlet water temperature, (2/7/2020). 63

Fig. 5.18: Hourly variation in solar irradiance during testing days. 64

Fig. 5.19: Hourly variation in wind speed during testing days. 65

Fig. 5.20: Hourly variation in ambient temperature during testing days. 65

Fig. 5.21: Hourly variation of water outlet temperature during testing days. 66

Fig. 5.22: Hourly variation of air outlet temperature during testing days. 67

Fig. 5.23: Hourly variation of useful energy for air part for testing days. 68

Fig. 5.24: Hourly variation of useful energy for water part for testing days. 68

Fig. 5.25: Hourly variation of efficiency for testing days. 69

Fig. 5.26: Water temperature difference.	70
Fig. 5.27: Air temperature difference.....	71
Fig. 5.28: Hourly efficiency of DPSC.....	72
Fig. A.1: Calibration of solar radiation meter	A-1

NOMENCLATURE

Symbol	Definition	Unite
A_c	The area of solar collector	m^2
C_p	Specific heat coefficient	J/kg.K
C_{-pw}	specific heat coefficient for water	J/kg.K
d_i	Inside diameter of pipe	m
d_o	External pipe diameter	m
f	The factor of friction	Dimensionless
G_T	Global radiation	W/ m^2
h	Coefficient of heat transfer	W/ m^2 . K
h_i	Internal convective heat transfer coefficient	W/ m^2 . K
h_c	Coefficient of heat transfer by convective	W/ m^2 . K
h_r	Coefficient of heat transfer by radiation	W/ m^2 . K
Symbol	Definition	Unite
h_w	The wind loss coefficient	W/ m^2 . K
I_T	Total solar irradiance	W/ m^2
k	Constant of thermal conductivity	W/ m. K
k_e	Thermal conductivity of insulation at edges	W/ m. K
k_b	Thermal conductivity of insulation at the bottom	W/ m. K
k_p	Thermal conductivity for absorber plate	W/ m. K
k_w	Coefficient of thermal conductivity for water	W/ m. K
K	Extinction coefficient	m^{-1}
L	Collector length	m
l	Distance between plate and covers	m
\dot{m}	The flow rate of mass	Kg/sec
Nu	Nusselt number	Dimensionless
Q	Thermal energy	W
Q_u	Useful thermal energy	W
t	The thickness of the twisted tape	m
T_{-amb}	Ambient temperature	$^{\circ}C$
T_{-out}	Temperature of outlet	$^{\circ}C$
T_{a_out}	Temperature of outlet air	$^{\circ}C$
T_{w_out}	Temperature of outlet water	$^{\circ}C$

$T_{num.}$	Temperature of numerical simulation	$^{\circ}C$
$T_{exp.}$	Temperature of experimental	$^{\circ}C$
T_p	Temperature of plate	$^{\circ}C$
T_{pm}	Mean plate temperature	$^{\circ}C$
Greek Symbols		
β	The tilt angle of the collector	Degree
ε_p	The emissivity of plate	Dimensionless
ε_c	The emissivity of glass (cover)	Dimensionless
η	collector efficiency	Dimensionless
ρ_w	Density of working fluid(water)	Kg/m^3
ν	kinematics viscosity of air	m^2/sec

DIMENSIONLESS GROUP

Symbol	Description
N	The number of covers(glass)
Nu	Nusselt number
Pr	Prandtl number
Ra	Rayleigh number
Re	Rynolds number
DPSC	Dual Purpose Solar Collector
FPSC	Flat plate solar collector

CHAPTER ONE

INTRODUCTION

CHAPTER ONE

INTRODUCTION

1.1 Renewable energy

In the light of this accelerating development and the global hunger for energy, because of the environmental problems produced by fossil fuel energy, as global warming problems and others. It is necessary to search for alternative sources that environmentally friendly and sustainable energy. Renewable energy swept through the research space and scientific interest for decades. Much attention has been focused on the aftermath of the massive economic crisis in fuel [1]. The world started thinking more seriously for the success of the work on renewable energy and increase its efficiency to be a substitute for high-energy fossil fuels Renewable energy sources are never implemented. It is distributed over very wide geographical areas. These resources are rapidly replenished by the natural process of the universe and it will not leave problems in the environment. The main advantage of using renewable energy is they are available at all times of the year [2].

1.1.1 Advantage of renewable energy [3]

- A- The most important renewable energy advantage is a sustainable energy and does not implement.
- B- It produces very little or no residue, such as carbon dioxide or other chemical pollutants.
- C- Renewable energy requires less maintenance than conventional generators.
- D- Renewable energy projects are more economically beneficial.
- E- Less labor requirements.

F- Take up less area than conventional power plant especially geothermal stations.

1.1.2 Disadvantage of renewable energy

- a. Renewable energy cannot produce the same quantity of energy as fossil fuel stations.
- b. The productivity of renewable energy is dependent on the weather as the source of this energy such as wind and sun.
- c. The current cost of renewable energy is high considering as a new technology.
- d. One of the disadvantages of renewable energy is that it is not possible in supporting a lot of technology such as air transport.

1.1.3 Types of renewable energy [2]

- a. Solar energy.
- b. Wind energy.
- c. Biomass power.
- d. Tidal power.
- e. Geothermal.
- f. Hydro power.
- g. Photovoltaic cells.

1.2 Solar energy

The sun is an extremely hot gaseous sphere with a diameter of $1.39 \times 10^9 m$. The black body temperature of the sun is 5760 K. The sun is an inexhaustible source of free energy. The total power output of the sun is $3.8 \times 10^{20} MW$, which is equal to $63 MW/m^2$ the surface of the sun. In all directions, this force radiates outward. The earth receives only a small fraction of the total released radiation, equal to $1.7 \times 10^{14} kW$, so, it goes without saying that we think well about how to invest this massive free energy. New technologies are used to generate electricity or heat from solar energy collected.[4]

Solar energy is the oldest renewable energy forms of humans since the time of a decent. The first application of this type was discovered in the south of France dating back to 8000 BC, Where a seat is used to the agricultural products during the excavations. Many locations are discovered in the Middle East where the material is diligent by solar energy, such as animal skins and clay for building writing.[5]

Complete solar radiation on the surface of the earth consists of direct radiation, diffuse radiation and reflected radiation. Direct radiation also known as beam radiation, this arrives from the Sun uni-directionally; diffuse radiation is Omni-directional due to molecular or suspended atmospheric dispersion. Reflected radiation, which results from the reflection of solar radiation from the Earth’s surface, is incidence on devices that tilt at an angle greater than 0° from the horizon. [6]

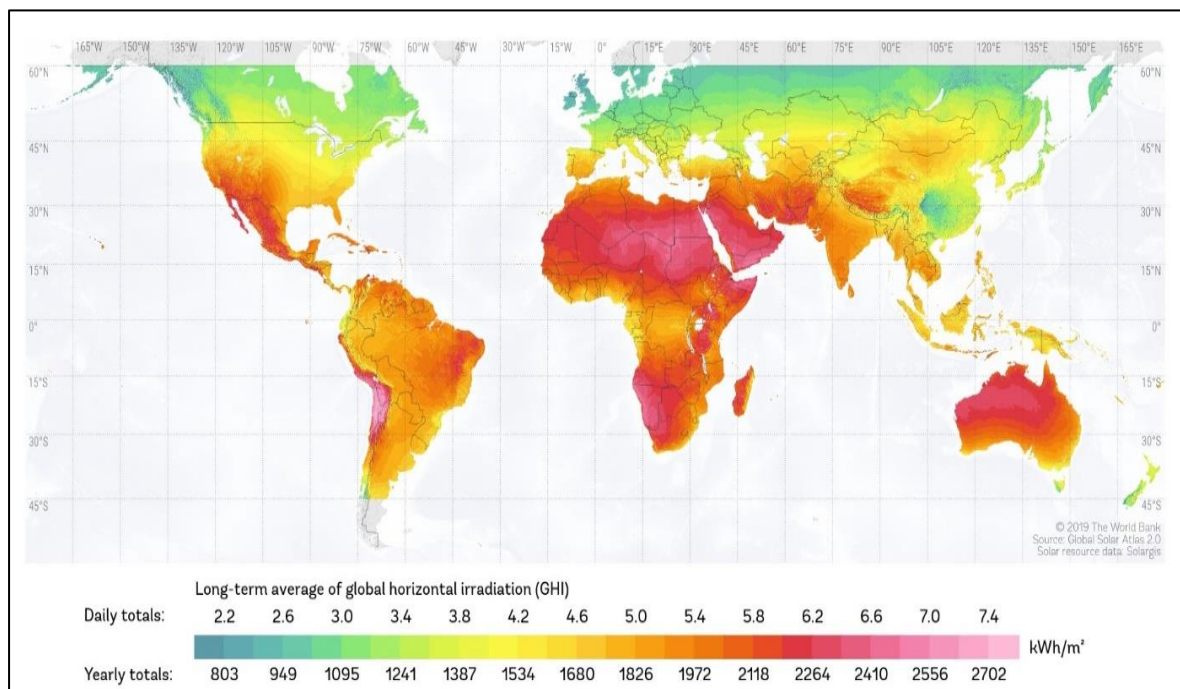


Fig. 1.1: The global solar radiation in World 2019.[7]

Figures (1.1 & 1.2), shows the distribution of the solar radiation in the world and Iraq [7]. Note the intensity of solar radiation in Iraq, which is a major reason for serious use of this energy.

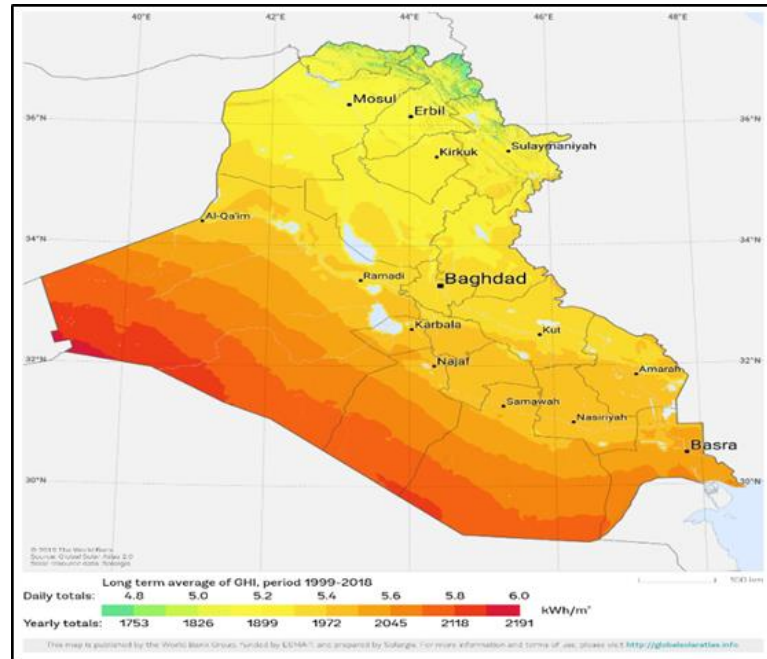


Fig. 1.2: The global solar radiation in Iraq 2019.[7]

The radiation of the Sun travels through the atmosphere of the earth, the intensity of the radiation decreases because of:

- a. Reflection from the atmosphere.
- b. Scattering of particles of dust and air waste.
- c. Air molecules scattering.

When the radiation hits a body, it reflects part of this radiation, part is absorbed. The reflected fraction of incident radiation is known as the reflectance, $\rho_{\text{reflectance}}$ the fraction of absorbed radiation as absorptance, $\alpha_{\text{absorptance}}$ and the fraction of transmitted radiation as transmittance, $\tau_{\text{transmittance}}$. [8]

1.3 Solar thermal collector

Solar energy collectors are special types of heat exchangers that convert the energy of solar radiation into the transport medium's internal energy. It is a system that absorbs the solar radiation coming in, transforms it into heat,

and transfer heat to a fluid that flows through the collector(usually air, or water) [4]

In several ways, the solar collector varies from many traditional heat exchangers. Typically, the latter exchange fluid to fluid at high heat transfer rates and with radiation as a consideration of no significance. In the solar collector, the transfer of energy from a remote source of radiant energy to fluid. At best, the density of incident radiation is about 1100 W/m^2 . [3]

Solar collectors absorb two forms of solar radiation; either non-concentrated or concentrated radiation as shown in figure 1.3. The area of the collector is the same as the area of the absorber for non-concentrated radiation, whereas in the concentrated radiation the collector area is greater than the absorber area. [9]

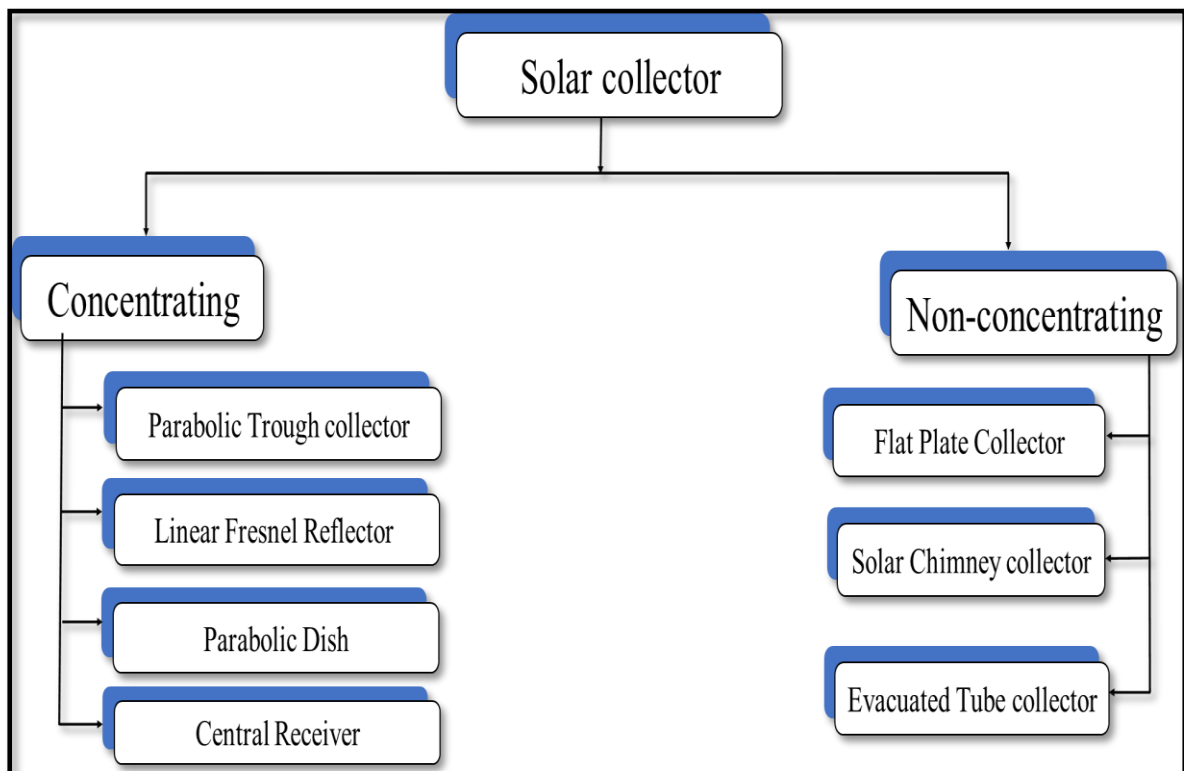


Fig. 1.3: Solar collector types. [3]

1.3.1 Flat plate solar collector (FPSC)

FPSC it is one of the most common and used types. An un- concentrated collector type can be provide for average temperatures of up to 100 C above ambient temperature. FPSCs have the benefits of being cheap to manufacture, all beam and diffuse radiation are collected, and they are permanently fixed in place, so there is no need to track the sun.[4]

These units ' main applications include solar water heating, building heating, air conditioning, and industrial process heat. Initially the solar collector is used for a single purpose, either to heat air or heat water. Some changes are made to the design of the collector to make it dual-purpose, i.e. used to heat air and water simultaneously. This modification reduce the cost and require space until 50% and provide more efficiency than single purpose. [10]

1.3.2 Components of dual purpose solar collector

The dual purpose solar collector (DPSC) as shown in figure 4 consist of the following components which are listed below: [11]

- a. Glass cover: One or more sheet of glass has been commonly used for glazing solar collectors, since it can relay as much as 90% of the solar irradiation in the short wave
- b. Fluid passageway: Tubes, fins, or channels that conduct or direct the inlet-to-outlet heat transfer stream.
- c. Absorber plate: Corrugated plates that are attached to channels. The embedded repair is a standard connection form. The plate is usually covered with a low-emittance film of high absorption.
- d. Pipes and channels: To admit and discharge the fluid.
- e. Insulation: Used to reduce heat loss from the collector's back and sides.

- f. Container: The case covers and protects the above parts from dust, dirt, and any other material.

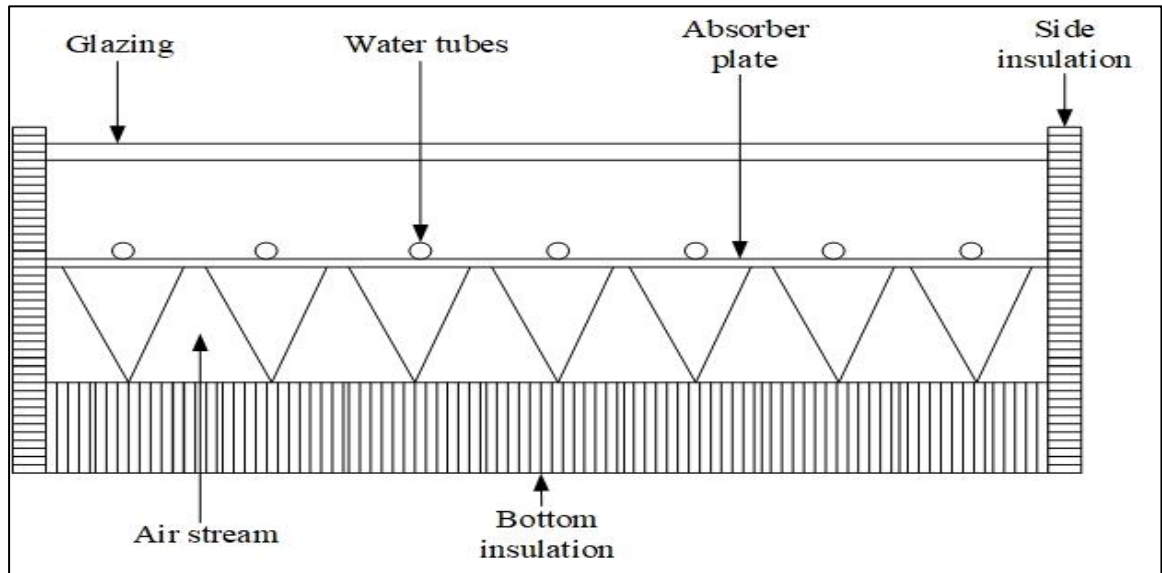


Fig. 1.4: Component of DPSC.[10]

1.3.3 Application of dual purpose solar collector

Dual-purpose solar collectors are characterized by being used to produce hot water and air at the same time. Using these collectors reduces space and cost by 50% [12]. Heated air or water produces from the dual purpose solar collector can be employed to different application as listed below: [3]

- a. Space heating for warehouses, factories, and building.
- b. Solar water heating for different applications.
- c. Air condition processes.
- d. Drying processes.

1.4 Research objectives

This study focuses on the forced convection circulation in the dual purpose solar collector. The following goals have been set:

- a. Simulation the heat transfer in absorber plate by using Comsol Multiphysics 5.5 software program.
- b. Validation the new proposal of absorber plate with previous study.
- c. Manufacture and testing of the proposed dual-purpose solar collector.
- d. Studying the effect of solar irradiance, water volumetric flow rate, inlet water temperature and air outlet velocity on performance of collector.

CHAPTER TWO
LITERATURE REVIEW

CHAPTER TWO

LITERATURE REVIEW

2.1 Introduction

Solar thermal collectors can be classified into to three groups based on their use: solar air collectors, solar water collectors, and dual-purpose solar collectors. In this chapter we will examine the most important studies that have been presented within this classification of solar collectors.

2.2 Studies about the solar air collectors

There are many studies that discussed development of performance of the solar air heater collectors, and we are going to summarize some of these studies. **K. Pottler et al.**[13] Conducted a study to improve the efficiency of the solar air collectors by letting the air passes behind the absorber plate to increase the energy gained from the collector. The study included the use of three different collectors with different arrangements of fins. Offset strip fins, continuous fins, and fin-free collectors were used in the study. It was found that the continuous fins collector provided the highest energy gain over the other two types of collectors with the optimal fin spacing of 5 – 10 mm. The study also showed that large offset strip fins provided good results, but the energy gained is always less than the energy gained from the optimally spaced continuous fins.

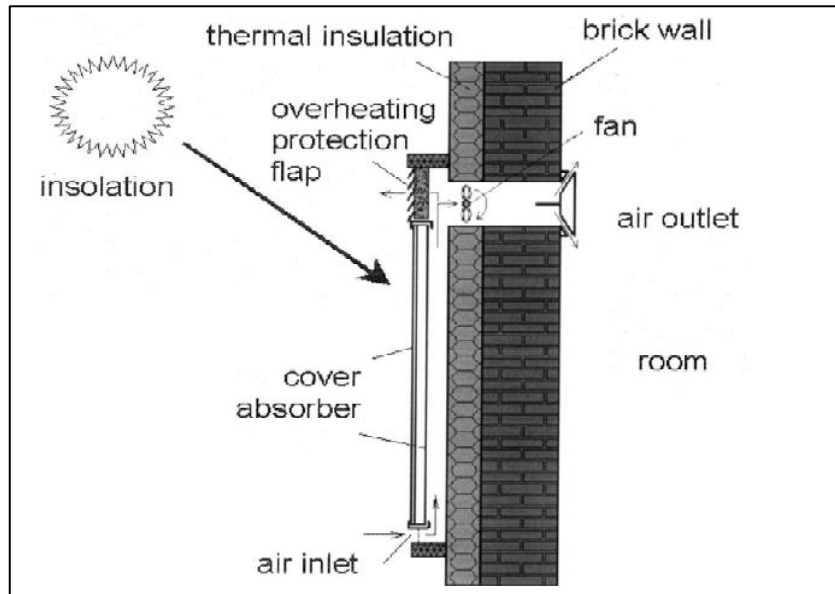


Fig. 2.1 Solar air collector system.[13]

P. Naphon [14] Carried out a theoretical study of the effect of double-pass. The study included the heat transfer property and performance of flat plate collector with and without porous media. The porous medium put in Air pass flow. The results comparing with previous researchers to validation it. The Authors concluded that the porous medium increases the efficiency by 25.9%. The difference between results of this study and previous study as 18.4% and 4.3% with and without porous respectively. The efficiency obtained is 50%. **M. A. Karim and M. N. A. Hawlader** [15] Carried out an experimental and mathematical study to compare the efficiency of the v-corrugated air collector over the flat plate collector. The results shows that the v-corrugated are 12% more efficient than the flat plate collectors, and the recommended flow rate for drying purposes is $0.035 \text{ kg/m}^2\cdot\text{s}$. The efficiency increases from 0.41 at $0.01 \text{ kg/m}^2\cdot\text{s}$ flow rate to 0.71 at $0.054 \text{ kg/m}^2\cdot\text{s}$ flow rate.

H. Esen [16] Carried out an experimental study analysis of energy and exergy of the double-pass flat plate collector with obstacle. The air flow through two passes, top and down absorber plate. The study show that the double-pass increasing the heat transfer area, therefore, increasing of

efficiency. **M. Mohanraj and P. Chandrasekar** [17] Conducted an experimental study on a flat panel solar air collector consists of a black-painted copper absorption plate, a thermal storage unit, and a glass cover. The distance between the absorption plate and cover is 25 mm and the tilt angle of the collector is 25°. The collector is designed so the air passes between the absorber plate and the glass cover. The system also includes a drying chamber which is used to dry chili. The drying rate depends on several factors: the solar radiation, ambient temperature, wind speed, relative humidity, and primary humidity rate. The experiment also included the use of heat storage materials (e.g., gravel) to exchange the heat with the system. It was concluded that the use of heat storage materials increases the drying time up to 4 hours a day and the rate of the collector efficiency by 21%. **Akpinar and F. Koçyiğit** [18] Published an experimental study of fourth types of flat plate solar air collector; three types with different obstacle and one type without obstacle. The first and second laws of efficiency was studied. The study showed that the two efficiency depend on solar radiation, geometry of absorber plate, and air flow line. Tests were held at two air mass flow, 0.0052 and 0.0074 kg/s. The values of first and second laws were 20-82% and 8.32-44% respectively. **K. Aoucs et al.** [19] Published an experimental and theoretical study of a solar air flat plate collector with obstacle rows in the dynamic air vein to enhance thermal efficiency. They made a comparison between the theoretical and experimental results, and found that the theoretical approach reflects in a satisfactory way the thermal performance of the tested prototype and the effects of its components, primarily the absorber, on the results achieved.

Tyagi et al.[20] Conducted an experimental study to analyses energy and exergy of flat plate collector with thermal storage material; paraffin wax and hytherm oil. They calculated first and second laws of efficiency with and

without the thermal storage material. The Authors concluded that the efficiency; without thermal storage material; increases with time until maximum value at noon then it reduces and with this material, the efficiency will increase until 4:30 pm. **S. M. González et al.** [21] Carried out an experimental and theoretical study of the behavior and efficiency of a counter-flow double-pass air heater. The prototype is tested during four sunny winter days with a maximum solar irradiance of 1100 W/m^2 and dry temperatures ranging from 8°C to 23°C . Outlet air temperature during the test reached 80°C at noon by using a resistor and 75°C without it. The average difference between the inlet and outlet temperatures was 40°C where the air flow was fixed at 0.02 kg/s . The average efficiency was 42% and peaking at 50%. [22] Conducted a theoretical and experimental study on the finned solar air collectors in regards to the tilt angle, and the flow and the inlet mode of the air. The study showed that the efficiency difference resulted is only 3% when changing the installation angle of the collector, which means that the angle has a little effect on the efficiency; while the flow showed to have a positive impact on the efficiency of the collector, especially when the flow is small and increases gradually. **C. Sun et al.**[23] Performed a mathematical and experimental analysis of a solar air collector consisting of two air passage channels, and a glass cover. The authors studied the effect of the flow rate on the efficiency of the collector under different conditions and forced convection. Mathematical analysis included air ducts, absorption plate, glass cover, thermal insulation board, and fan energy. They found that when the mass flow rate increases the hydraulic thermal efficiency will increase until it reaches a certain rate then it starts decreasing, but the outlet air temperature decreases as the mass flow rate increases; however, the effect of the ambient temperature on the efficiency will increase as the flow rate increases. These results were useful to design and analyze future solar collectors.

A. A. Razak et al. [24] published a study on the most popular absorber plate designs for the solar air collectors. The study focuses on the contemporary improvements on the thermal performance of the collectors and primarily on the available absorption materials for the matrix air collectors. It is showed that the matrix air collectors have the most potential for improvement and are more efficient than the other types of collectors. The study also noted that the matrix air collectors are given the least attention compared to the other types. The performance of the matrix collector is strongly affected by several factors such as the matrix porosity, geometry, thickness, surface area density, and material thermal properties. But the parameters which is useful for energy efficiency for the other types of collectors such as including fins and flow direction gave negative results on the energy efficiency of the matrix air collectors. [25] Included a theoretical and experimental study to compare the efficiency of the rectangular-finned air collectors and the fin-free air collectors. While keeping the mass flow rate fixed at 0.033 kg/s, they proved that including the fins reduced the Nusselt number from 19.67 to 16.23, reduced the hydraulic diameter, increased the heat transfer coefficient between the absorber plate and the air, reduced the thermal losses, and increased the outlet temperature. Experimental efficiency is found to be 30% for the fin-free collector and 51% for the finned collector, while the theoretical efficiency is found to be 33% for the fin-free collector and 55% for the finned collector. [1] Carried out an experimental study on flat plate solar air collector to reduce the thermal losses. The collector consists of a black-coated steel absorption plate, and double layers of glass. The inclination angle of the collector is 37°. The results of adding the second glass layer and changing the distances between the two glass layers at 1, 2 and 3 cm were compared with the results of having single glass layer, and it was found that adding the second glass layer was effective in reducing the

thermal losses. **A. Fudholi and K. Sopian** [26] Published a study to discuss the fundamental mechanisms of the solar collectors and their performance, and discuss and summarize the theoretical and experimental results of the previous studies done on the solar air flat plate collector. During indoor testing, the energy and exergy efficiencies of solar air flat plate collectors range from 30% to 79% and from 8% to 61%, respectively. While the energy and exergy efficiencies of the solar air flat plate collector in the drying application (outdoor testing) range from 28% to 62% and from 30% to 57%, respectively.

2.3 Studies about the solar water collectors

The second type of solar collectors are solar water heater collectors. The following researchers investigate in this kind. **Kumar and Rosen** [27] Carried out a theoretical study to analysis thermal performance of solar water heater with corrugated absorber surface. The thermal performance of collector is depend on the heat transfer rate between absorber and water, and amount of incident solar radiation. The results show that the outlet water temperature of corrugated absorber is higher than plane surface. . **H. Martín et al.** [28] Published a theoretical study of heat transfer enhancement by using wire-coil inserts inside the water tube. The authors using TRNSYS as a simulating tool. The methodology of numerical simulation predicts the thermo hydraulic flow behavior of enhanced and standard tube-on-sheet solar collectors, evaluated heat loss, friction coefficient and Nusselt number as a function of operating parameters. The author's conclusion is that the efficiency increases by 4.5%.

S. Hossain et al.[29] Conducted an experimental study to enhance the efficiency of the flat plate solar water collector by rearrange pipes. The new arrangement is two parallel rows. It has a higher convective heat transfer

between absorber and water, and more surface area exposed to solar radiation. The new suggestion design advantages are that easy to instillation, less cost and high thermal efficiency. The results show that the average of 75.50% for two months and the outlet temperature of 98°C. **J. Zhao** [30] Published an experimental and theoretical study to analysis the effect of the maximum daily heat energy collected and flow rate on the daily heat energy under conjunction the solar collector and tank. This study also proposed a simplified formula for computing the daily heat energy collected. The results show that the optimum flow rate is 0.005 kg/m².s for stable daily collected heat energy.

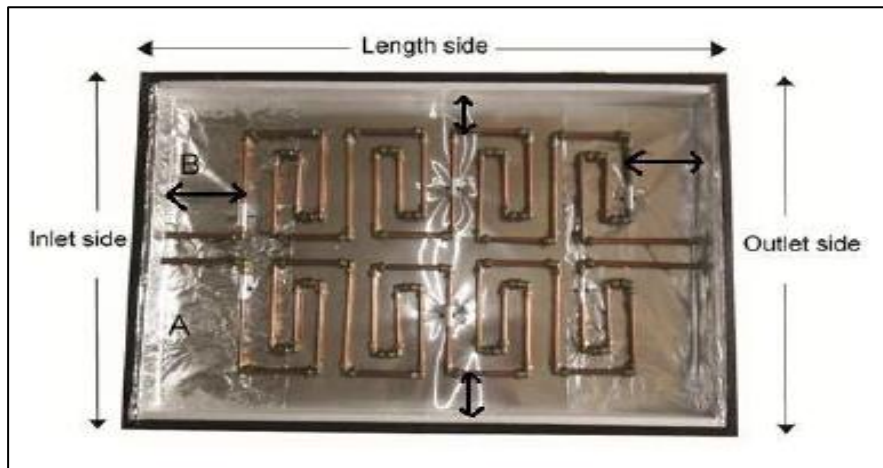


Fig. 2.2: Copper pipes arrangement inside the wood box. [30]

Z. Wang et al. [31] Carry out a review paper common solar water heater with phase change material. This study conduct two sides, structural characterization and research methodology. This work helps to identify the potential research to improvement of the efficiency of the system. **S. K. Verma et al.** [32] Conducted an experimental study for testing performance of flat plate solar water collector with Mgo/ water working fluid with particle size ~40 nm. The study included effect of mass flow rate and particle volume fraction on the efficiency of the collector. The results show that used Mgo/water Nano fluid increases the efficiency comparison with water

as working fluid by 9.34%. **K. Balaji et al.** [33] Published a theoretical study to analysis thermal performance of extended surface of absorber tubing of flat plate solar water collector by using passive technique. This technique based on changes the geometry of flow path of fluid. The objective of this study is increases effective of the heat transfer coefficient with minimum pressure drop. Two type of velocity enhancer were used in this study, then compared work at rod and tube. The authors concluded that the rod velocity enhancer greater than the tube velocity enhancer and the increase in efficiency are 15% and 10% for rod and tube respectively. **D. G. Gunjo et al.** [34] Conducted an experimental and theoretical study. This study investigate the effect of inlet water temperature, ambient temperature, solar radiation, and mass flow rate on the outlet temperature and thermal efficiency. The numerical analysis based on (CFD) with single riser tube and absorber plate at steady state. Thermal efficiency increases with increases water flow rate, solar radiation, ambient temperature, while, reduces with inlet water temperature.

Deeyoko et al. [35] Published an experimental and theoretical study to enhancement the convective heat transfer coefficient by increasing the effective area between the heat transfer liquid and the contact surface area. Rectangular and square fins were used to enhancement the thermal performance of the collector. The results show that the rectangular fin gives more energy and exergy efficiency. The rectangular fin efficiency is higher than plain tube by 18-20% at different mass flow rates. The square fin efficiency less than rectangular fin by 3-5%.

2.4 Studies about the dual-purpose solar collectors

The new design of flat plate solar collector is used to heat air and water simultaneously. The following researchers are students in this type. **Assari et al.** [36] Design and study experimentally and theoretically of the dual solar collector. Different tests are done to investigate dual solar collector efficiency and outlet temperature or both fluids. Theoretical results showed a good agreement with experimental results. The results show that the minimum flow rate can be given highest temperature and efficiency. The air part with triangular channel can be provide increment in efficiency and temperature about 10% in comparison with other collector type such as V-corrugated.. **Assari et al.** [10] Studied an experimental and theoretical investigation performance of dual purpose solar collector (DPSC). Two fluids are flow in this collector simultaneously to product hot air and hot water. Experimental data show that high temperature and high performance can be obtained by using this collectors compared to single solar collectors. Effectiveness method used to investigate thermal performance of DPSC mathematically. Three different type of air duct are used to enhance the performance of collector, such as rectangular fin, triangular fin and without fin. The results shown that the rectangular fin have better performance compared with other and heat delivery decreases as water inlet temperature increases.

J. Ma et al. [11] Published an experimental and theoretical study of the efficiency of a dual solar collector. The system will increase annual thermal conversion ratio of solar energy. This collector modifying from conventional solar water heater with absorber plate fins are L-shaped to increase the heat transfer in air heating part. The experiment results show that the collector can be increase the temperature of 100 L by 30° C or a whole day by using this type of solar collector. In water heating, the daily

efficiency reached 50%. While the daily efficiency of air heating reached 52%. **A. V. AK and P. Arun** [37] Conducted a numerical simulation study on the performance enhancement of a dual purpose solar collector integrated with porous matrix. The simulation is carry out by ANSYS 13 software program. The suggestion system is compared with dual solar collector designed by M.R. Assari, et al. [10] The simulation results show that significantly higher temperature rise is obtained for air and water streams under various operating conditions as compared to the original system without the porous medium.

Mohajer et al. [38] Carry out an experimental study on same collector which design by M.R. Assari et al. [10] but in this study, The Authors studied dray a mixture of vegetables (parsley, dill and coriander) at constant air and water flow rates. Besides, the results were compared to the ones obtained when an electrical heater was applied in the solar drier as an auxiliary source for heating. The study show that the heater is used, temperature of trays increased by 20-30 C more than case without heater, but the heater will brings additional costs for electricity and reduce quality of products. The system without heater can be reduce costs and space about 50% in comparison with single purpose water or air heating. **R. Venkatesh and W. Christraj** [39] conducted an experimental study to increase the performance of solar collectors by investigate a dual-purpose solar collector. The testing of this system included as solar water heater and solar air heater simultaneously in two cases, with load and on load conditions. The results show that the efficiency of solar water heater is 67.69% at mass flow rate of 0.015 kg/s, while, the efficiency of solar air heater is 85.1% at mass flow rate of 0.0104 kg/s. The average of efficiency of multipurpose solar collector is 70%. **Omid et al.** [12] Published an experimental study to investigate the performance of single and dual purpose solar collectors. The study included

testing dual purpose solar collector at two different speeds of air, 2.8 and 3.2 m/s respectively. Using dual purpose solar collector decreases costs and required space. This study showed that the efficiency of dual purpose higher than single purpose by 3 to 5%. **D. Zhang et al.** [40] Studied flat plate solar collector experimentally and theoretically with three modes: (A) air heating, (B) water heating and (C) air-water compound heating. The mathematical model is analysis the effect of mass flow rate on performance for air and water heating modes. The average collector efficiency is 51.3% and 51.4% for mode A and B respectively. In mode C, the average thermal efficiency about 73.4%. Also, the results show that the mass flow rate effected significantly on thermal efficiency and outlet temperature. In mode A, the air mass flow rate between 0.02 kg/s and 0.25 kg/s is recommended and the water mass flow rate between 0.06 kg/s and 0.08 kg/s is recommended in mode B. **T. Rajaseenivasan and K. Srithar** [41] Studied dual solar collector experimentally investigation on humidification dehumidification system. The system consist of dual solar collector with semicircular convex and concave shape integrated with absorber plate to create the turbulence, and packed bed humidification dehumidification unit. The system was tested with varying the mass flow rate of air (0.84 to 1.08 kg/min) and water (1 to 3 kg/min). The dual purpose collector supplies the required hot water and hot air for desalination system. In this collector, Air flows over the top surface of the absorber plate and the water flows through the riser tubes, attached in the bottom side of absorber plate. The heated air and water from the collector is supplied to the humidifier, where the air gets humidified and moves towards dehumidifier for condensation. The capacity of system distillation enhances with the water and air temperature and flow rate of air, cold water and hot water. The authors concluded that the maximum distillate of 15.23, 14.14, and 12.36 kg/m².d is collected for the concave, convex and conventional system respectively. The total efficiency of the system increase about 68%

with the presence of tabulators in the collector. **J. Ma et al.** [42] Carried out an experimental and theoretical study to investigate dual function solar collector (DFSC) integrated with building. The experimental study conducted at two conditions: controlled indoor temperature and non-controlled. The numerical results were validated with the experimental results. The experimental show that the temperature of room can be increase by 3.43°C in winter due to using DFSC and power consumption of 3.5 KWh when the room temperature set at 18°C. The numerical results show that mean daily efficiency of dual function solar collector was 44.3%.

From the above it is noticed that the most studies focused on studying the effect of design of absorber plate or air passage or water pipes distribution separately. In this present work, the effect of absorber plate design and water pipes distribution were studied together. The new type of absorber plat is a corrugated plate with zig-zag water pipes. The effect of this new type under different weather condition and many parameters, have been studied numerically and experimentally.

2.5 Summary

Table 2.1 shows the summary for this chapter:

Table 2-1: Literature review summary.

Researcher name	Year	References	Collector's type	Research type	Results summary
Pottler et al.	2000	[13]	Air heater	experimental and mathematical	<ul style="list-style-type: none"> • Large offset strip fins provided good results, but the energy gained is always less than the energy gained from the optimally spaced continuous fins.
Naphon	2005	[14]	Air heater	theoretical	<ul style="list-style-type: none"> • The porous medium increases the efficiency by 25.9%. • The difference between results of this study and previous study as 18.4% and 4.3% with and without porous respectively.
Karim & Hawlader	2006	[15]	Air heater	experimental and mathematical	<ul style="list-style-type: none"> • The v-corrugated are 12% more efficient than the flat plate collectors. • The recommended flow rate for drying purposes is 0.035 kg/m².s.
Esen	2008	[16]	Air heater	experimental	<ul style="list-style-type: none"> • The double-pass increasing the heat transfer area, therefore, increasing of efficiency.

Mohanraj & Chandrasekar	2009	[17]	Air heater	experimental	<ul style="list-style-type: none"> the use of heat storage materials increases the drying time up to 4 hours a day
Akpınar and Koçyiğit	2010	[18]	Air heater	experimental	<ul style="list-style-type: none"> The values of first and second laws of efficiency were 20-82% and 8.32-44% respectively.
Aoucs et al.	2011	[19]	Air heater	experimental and theoretical	<ul style="list-style-type: none"> The theoretical approach reflects in a satisfactory way the thermal performance of the tested prototype and the effects of its components, primarily the absorber, on the results achieved.
Tyagi et al.	2012	[20]	Air heater	experimental	<ul style="list-style-type: none"> The efficiency; without thermal storage material; increases with time until maximum value at noon then it reduces and with this material.
González et al.	2014	[21]	Air heater	experimental and theoretical	<ul style="list-style-type: none"> The average difference between the inlet and outlet temperatures was 40°C where the air flow was fixed at 0.02 kg/s. The average efficiency was 42% and peaking at 50%.
Chang et al.	2015	[22]	Air heater	experimental and theoretical	<ul style="list-style-type: none"> The study showed that the efficiency difference resulted is only 3% when changing the installation angle of the collector. The flow showed to have a positive impact on the efficiency of the collector, especially when the flow is small and increases gradually.

Sun et al.	2016	[23]	Air heater	experimental and theoretical	<ul style="list-style-type: none"> • When the mass flow rate increases, the hydraulic thermal efficiency will increase. • The effect of the ambient temperature on the efficiency will increase as the flow rate increases.
Razak et al.	2016	[24]	Air heater	experimental and theoretical	<ul style="list-style-type: none"> • The matrix air collectors have the most potential for improvement and are more efficient than the other types of collectors. • The performance of the matrix collector is strongly affected by several factors such as the matrix porosity, geometry, thickness, surface area density.
Daliran and Ajabshirchi	2018	[25]	Air heater	experimental and theoretical	<ul style="list-style-type: none"> • The fins reduced the Nusselt number from 19.67 to 16.23, increased the heat transfer coefficient between the absorber plate and the air. • Experimental efficiency is found to be 30% for the fin-free collector and 51% for the finned collector
Chabane & Sekseff	2018	[1]	Air heater	experimental	<ul style="list-style-type: none"> • Adding the second glass layer was effective in reducing the thermal losses.

Fudholi and Sopian	2019	[26]	Air heater	experimental and theoretical	<ul style="list-style-type: none"> The indoor testing resulted from the study showed an energy and exergy efficiencies range from 30% to 79% and from 8% to 61% respectively. The outdoor testing (for drying applications) showed an energy and exergy efficiencies range from 28% to 62% and from 30% to 57% respectively.
Kumar and Rosen	2010	[27]	Water heater	theoretical	<ul style="list-style-type: none"> The outlet water temperature of corrugated absorber higher than plane surface.
Martín et al.	2011	[28]	Water heater	theoretical	<ul style="list-style-type: none"> The author's conclusion that the efficiency increases by 4.5%.
Hossain et al.	2014	[29]	Water heater	experimental	<ul style="list-style-type: none"> The new suggestion design advantages are that easy to instillation, less cost and high thermal efficiency. The average of 75.50% for two months and the outlet temperature of 98°C.
Zhao et al.	2014	[30]	Water heater	experimental and theoretical	<ul style="list-style-type: none"> The optimum flow rate by 0.005 kg/m².s for stable daily collected heat energy.
Wang et al.	2015	[31]	Water heater	experimental	<ul style="list-style-type: none"> This work help identify the potential research to improvement of the efficiency of the system.
Verma et al.	2016	[32]	Water heater	experimental	<ul style="list-style-type: none"> Used Mgo/water Nano fluid increases the efficiency comparison with water as working fluid by 9.34%.

K. Balajia et al.	2017	[33]	Water heater	theoretical	<ul style="list-style-type: none"> The rod velocity enhancer greater than the tube velocity enhancer and the increase in efficiency are 15% and 10% for rod and tube respectively.
Gunjo, Mahanta, and Robi	2017	[34]	Water heater	experimental and theoretical	<ul style="list-style-type: none"> Thermal efficiency increases with increases water flow rate, solar radiation, ambient temperature, while, reduces with inlet water temperature.
Anto Joseph Deeyoko et al.	2019	[35]	Water heater	experimental and theoretical	<ul style="list-style-type: none"> The rectangular fin gives more energy and exergy efficiency. The rectangular fin efficiency is higher than plain tube by 18-20% at different mass flow rates. The square fin efficiency less than rectangular fin by 3-5%.
Assari, et al.	2007	[36]	Dual-purpose	experimentally and theoretically	<ul style="list-style-type: none"> The minimum flow rate can be given highest temperature and efficiency.
Assari et al.	2011	[10]	Dual-purpose	experimental and theoretical	<ul style="list-style-type: none"> High temperature and high performance can be obtained by using this collectors compared to single solar collectors. the rectangular fin have better performance compared with other and heat delivery decreases as water inlet temperature increases

Ma et al.	2011	[11]	Dual-purpose	experimental and theoretical	<ul style="list-style-type: none"> • The collector can be increase the temperature of 100 L by 30° C or a whole day. • In water heating, the daily efficiency reached 50%. While the daily efficiency of air heating reached 52%.
AK and Arun	2013	[37]	Dual-purpose	theoretical	<ul style="list-style-type: none"> • Significantly higher temperature rise is obtained for air and water streams under various operating conditions as compared to the original system without the porous medium.
Mohajer et al.	2013	[38]	Dual-purpose	experimental	<ul style="list-style-type: none"> • When the heater is used, temperature of trays increased by 20-30 C more than case without heater, but the heater will brings additional costs for electricity and reduce quality of products.
Venkatesh and Christraj	2013	[39]	Dual-purpose	experimental	<ul style="list-style-type: none"> • The efficiency of solar water heater is 67.69% at mass flow rate of 0.015 kg/s, while, the efficiency of solar air heater is 85.1% at mass flow rate of 0.0104 kg/s. • The average of efficiency of multipurpose solar collector is 70%.
Omid et al.	2014	[12]	Dual-purpose	experimental	<ul style="list-style-type: none"> • Using dual purpose solar collector decreases costs and required space. • the efficiency of dual purpose higher than single purpose by 3 to 5%

Zhang et al.	2016	[40]	Dual-purpose	experimental and theoretical	<ul style="list-style-type: none"> • In mode A, the air mass flow rate between 0.02 kg/s and 0.25 kg/s is recommended and the water mass flow rate between 0.06 kg/s and 0.08 kg/s is recommended in mode B.
Rajaseenivasan and Srithar	2017	[41]	Dual-purpose	experimental	<ul style="list-style-type: none"> • The highest distillate of 15.23, 14.14, and 12.36 kg/m².d is collected for the concave. • The total efficiency of the system increase about 68% with the presence of tabulators in the collector.
Ma et al.	2018	[42]	Dual-purpose	experimental and theoretical	<ul style="list-style-type: none"> • The temperature of room can be increase by 3.43°C in winter due to using DFSC and power consumption of 3.5 KWh when the room temperature set at 18°C.

CHAPTER THREE
NUMERICAL SIMULATION

CHAPTER THREE

NUMERICAL SIMULATION

3.1 Comsol introduction

In this chapter, three dimensional heat transfer and unsteady incompressible flow have been solved by using COMSOL Multiphysics 5.5. The absorber plate, water outlet temperature, air outlet temperature, and glass cover temperature can found by COMSOL Multiphysics software. This software program was solved the different parameters by finite element method and many applied problems.

Simulation of computers has been become an integral aspect of research and engineering. In particular, digital component analysis is critical when designing new technologies or optimizing designs. A wide range of simulation solutions is available nowadays; researchers use everything from basic programming languages to numerous high-level modules that incorporate specialized methods. Although each of these strategies has its own distinctive characteristics, they all share a similar concern[43]

COMSOL Multiphysics is an integrated environment for solving time dependent or stationary second order processes in one, two, and three dimensional partial differential equations. It is a scalable framework where even beginner users can model all related physical aspects of their designs. Professional users can go further and use their experience to create tailor-made approaches that are specific to their particular situations. COMSOL needs that each form of simulation included in the kit should be capable of

being paired with each other. Currently, this stringent criterion mirrors what is happening in the real world.[43]

3.2 Building of model

In table 3.1 shows the parameters, symbols and dimensions of model that used in building the model in COMSOL environmental. The domain was divided into several parts, defined each part of its location in the system.

Table 3-1 Description, symbol and dimensional of model.

Description	symbol	Expression
pipe Radius	R_w	7[mm]
Curve pipe Radius	R_m	12.5 [cm]
Width of collector	W	100 [cm]
Height of collector	H	12.6 [cm]
Thickness of glass	t_g	0.6 [cm]
Length of collector	L	200 [cm]
height of water pipe	h_p	5[cm]
First pipe length	L_1	85 [cm]
Second pipe Length	L_2	70[cm]
step in x- axis	X_s	25 [cm]

iii. Air domain

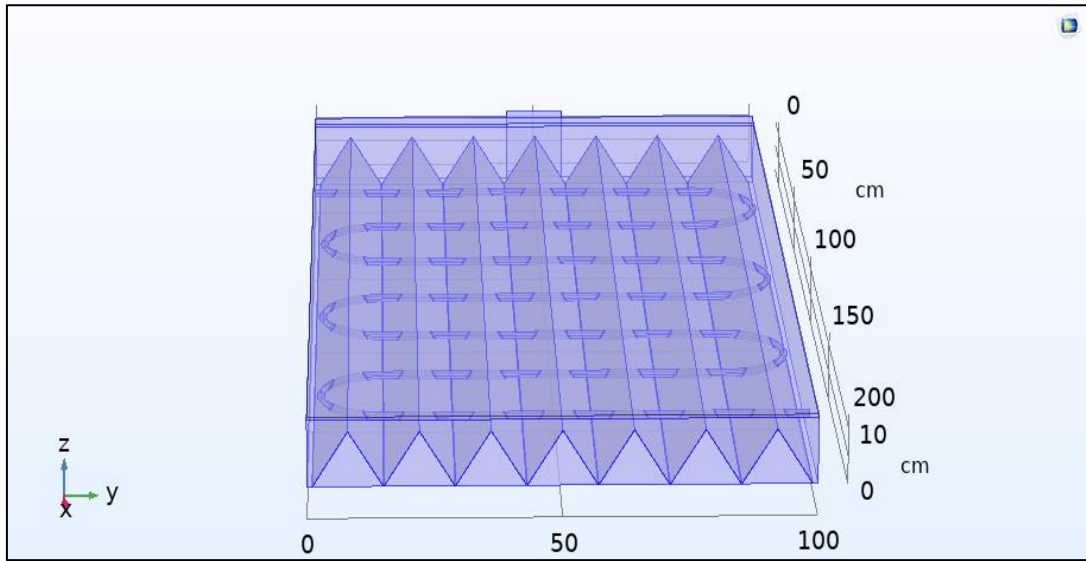


Fig. 3.3: Air domain.

iv. Glass domain

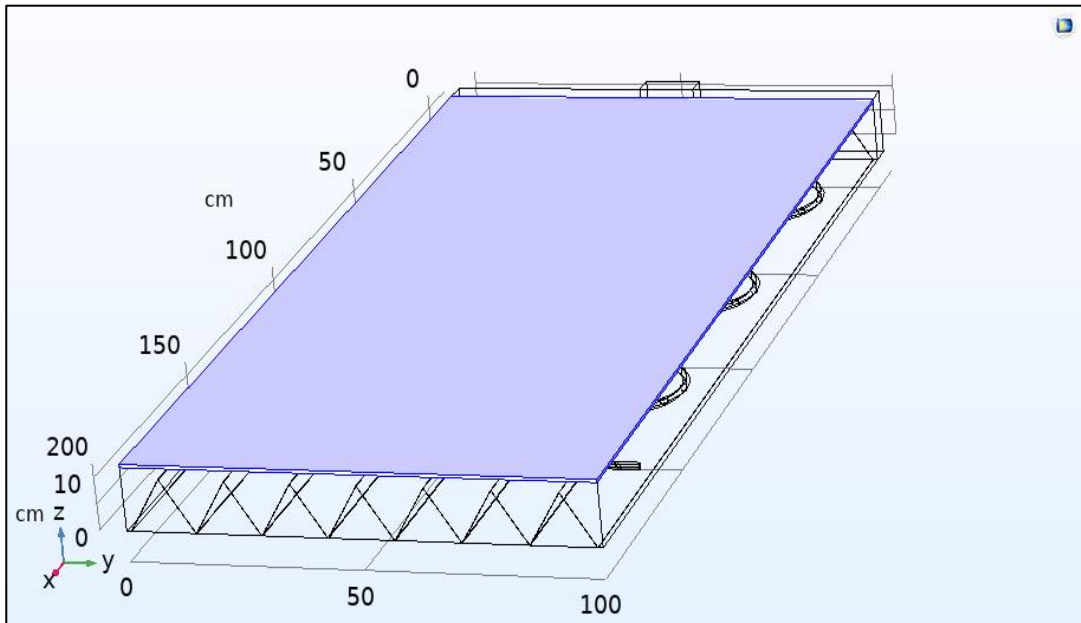


Fig. 3.4: Glass domain.

3.4 Physics of study

After defining the material that used in each part of the model, physics of model simulation are added according to the actual behavior. The model is exposed to several physics according to the assumptions that were adopted in simulation, laminar flow physics was chosen in the air and water domains. Physics of heat transfer was added to the model, the boundary conditions were defined for each domain as well as the initial values for the different inputs. The solar irradiance that hits on the collector surface was defined as heat flux.

3.5 Mesh generation

For complex geometries, high-quality unstructured mesh generation forms a major part of numerical simulation in different applications. Several mesh generating algorithms for complex 2D/3D domains were proposed and implemented successfully to solve various complex problems [44]. The type of mesh it was default type .It is well known that numerical methods accuracy and convergence depend on the shape and size of the mesh components as shown in figure 3.5.[45]

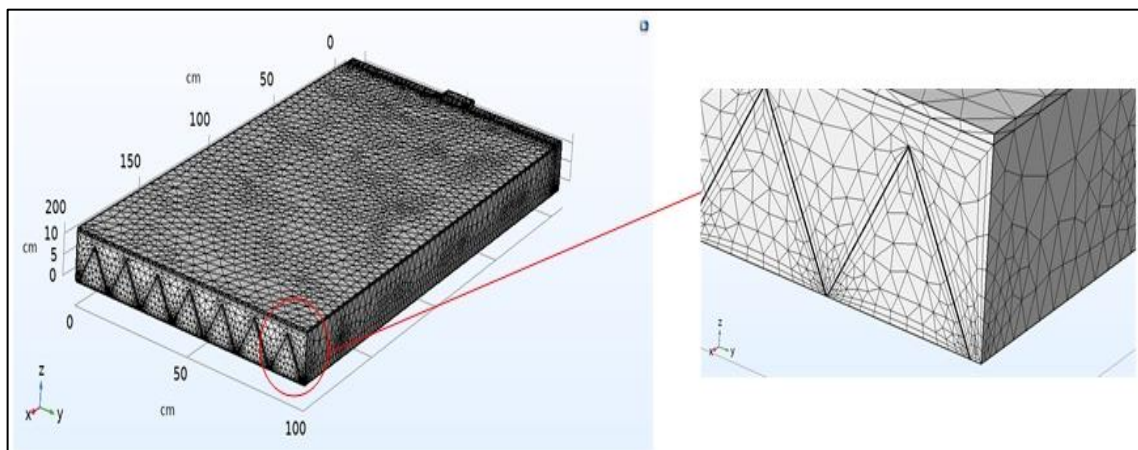


Fig. 3.5:Mesh generation.

3.6 Steps of numerical solution

Numerical solution is done by two parts; the first one; - by using computational fluid dynamics equations, eq. (3-1), (3-2), (3-3), (3-4) and (3-5). These equations are solved by using software program to calculate the absorber plate temperature (T_{pm}), water outlet temperature (T_{w_o}), air outlet temperature (T_{a_o}). These calculations are dependent on solar radiation (G), water inlet temperature (T_{wi}), ambient temperature (T_{amb}) and wind velocity (V).

All this input data are variable with time of Muthanna City/ Iraq. Where (G), T_{wi} , T_{amb} and V) values are taken from experiment data of present work.

The second one: - after found calculations of (T_{pm} , T_{w_o} and T_{a_o}) from numerical solution, now using equations (3-6), (3-7) and (3-8) to determine the thermal efficiency of collector mathematically.

Figure (3.6) below showing procedure of solution by COMSOL program.

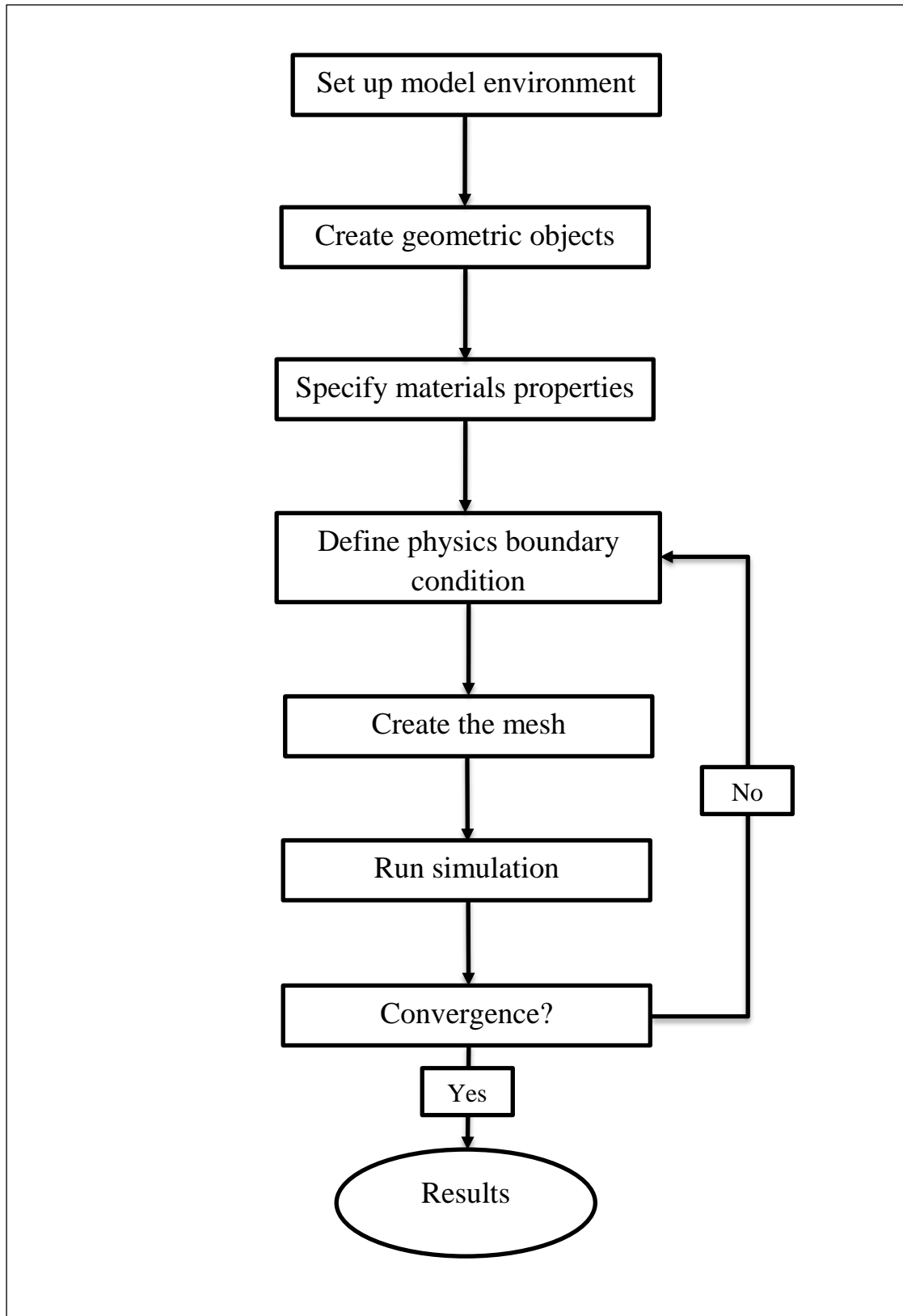


Fig. 3.6: Simulation methodology.

3.7 Assumption of model

The following assumptions are adopted in the proposed model simulation process:

- 1- The dual purpose solar thermal collector (DPSC) is 3-D unsteady flow.
- 2- There is no heat dissipation in the back and side surface.
- 3- Water flow in the pipes is laminar.
- 4- Air flow in the channels is laminar.
- 5- Radiation and conduction in the water pipes and air channels are assume negligible.

3.8 Mathematical of dual purpose solar collector (DPSC)

The equations using in the fluid flow is incompressible Navier-Stokes equations. The governing equations of modelled:

3.8.1 Covering equations

- 1- Mass Conservation Equation

$$\frac{\partial \rho}{\partial t} + \frac{\partial u}{\partial x} \rho + u \frac{\partial \rho}{\partial x} + \frac{\partial v}{\partial y} \rho + v \frac{\partial \rho}{\partial y} + \frac{\partial w}{\partial z} \rho + w \frac{\partial \rho}{\partial z} = 0 \quad (3-1)$$

Where ρ is fluid density (kgm^{-3}), \mathbf{u} is velocity vector (ms^{-1}).

- 2- Momentum conservation equation

- a- X- direction momentum equation

$$\frac{\partial u}{\partial t} + u \frac{\partial u}{\partial x} + v \frac{\partial u}{\partial y} + w \frac{\partial u}{\partial z} = -\frac{1}{\rho} \frac{\partial P}{\partial x} + \mu \left(\frac{\partial^2 u}{\partial x^2} + \frac{\partial^2 u}{\partial y^2} + \frac{\partial^2 u}{\partial z^2} \right) \quad (3-2)$$

- b- Y- direction momentum equation

$$\frac{\partial v}{\partial t} + u \frac{\partial v}{\partial x} + v \frac{\partial v}{\partial y} + w \frac{\partial v}{\partial z} = -\frac{1}{\rho} \frac{\partial P}{\partial y} + \mu \left(\frac{\partial^2 v}{\partial x^2} + \frac{\partial^2 v}{\partial y^2} + \frac{\partial^2 v}{\partial z^2} \right) \quad (3-3)$$

c- Z- direction momentum equation

$$\frac{\partial u}{\partial t} + u \frac{\partial w}{\partial x} + v \frac{\partial w}{\partial y} + w \frac{\partial w}{\partial z} = -\frac{1}{\rho} \frac{\partial P}{\partial z} + \mu \left(\frac{\partial^2 w}{\partial x^2} + \frac{\partial^2 w}{\partial y^2} + \frac{\partial^2 w}{\partial z^2} \right) \quad (3-4)$$

3- Energy conservation equation

$$\frac{\partial T}{\partial t} + u \frac{\partial T}{\partial x} = \alpha \frac{\partial^2 T}{\partial x^2} \quad (3-5)$$

4- (DPSC) efficiency

$$q_u = \varepsilon_f m_f c_{p,f} (T_{pm} - T_{fi}) \quad (3-6)$$

$$\varepsilon_f = \frac{m_f c_{p,f} (T_{f2} - T_{f1})}{m_f c_{p,f} (T_{pm} - T_{f1})} = \frac{(T_{f2} - T_{f1})}{(T_{pm} - T_{f1})} \quad (3-7)$$

$$\eta = \frac{q_u}{A_p I_T} \quad (3-8)$$

3.8.2 Boundary condition

The boundary conditions are listed below:

- i. Inlet water: $u=0$, $v=0$, $w=w_i$, $T=T_{wi}$.
- ii. Inlet air: $u=0$, $v=0$, $w=w_i$, $T=T_{amb}$.
- iii. Outlet water: $u=u_{out}$, $w=w_{out}$, $T=T_{out}$.
- iv. Outlet air: $u=u_{out}$, $w=w_{out}$, $T=T_{out}$.

CHAPTER FOUR
EXPERIMENTAL WORK
AND MEASUREMENTS

CHAPTER FOUR

EXPERIMENTAL WORK

4.1 Introduction

In this chapter, the experimental work will be explained. This section will be divided into three parts: the first part illustrates the construction, material and parts of solar flat plate collector, the second part elucidates measurements tools and the third part shows the rig specification and experimental procedure.

4.2 Experimental rig

The dual purpose solar collector system consist of several devices to conduct certain functions. The main part of the system is a dual purpose solar flat plate collector (DPSC). The water tank that is placed besides the collector. Electric air fan that is pulls the air through the channels. An electric pump using to circulating water inside the system. The flowmeter is installed after the water pump to control the water flow rate and it is controlled by valves. The supply and return water pipe are connected between water tank and collector. Figure 4.1 showed a photo for the dual purpose solar collector system with measurement devices.



Fig. 4.1: Photo for DPSC system with measurment devices.

4.2.1 Dual purpose solar collector

The dual-purpose solar is easy to manufacturing from materials made available locally, cheap and require less maintenance than other type. The modification type used to supply hot water and hot air simultaneously. It is power unit in the system. By using solar collector, the solar energy is transformed into heat energy and passed to the working fluid. Figure 4.3 showed the essential parts of dual-purpose solar flat plate collector.

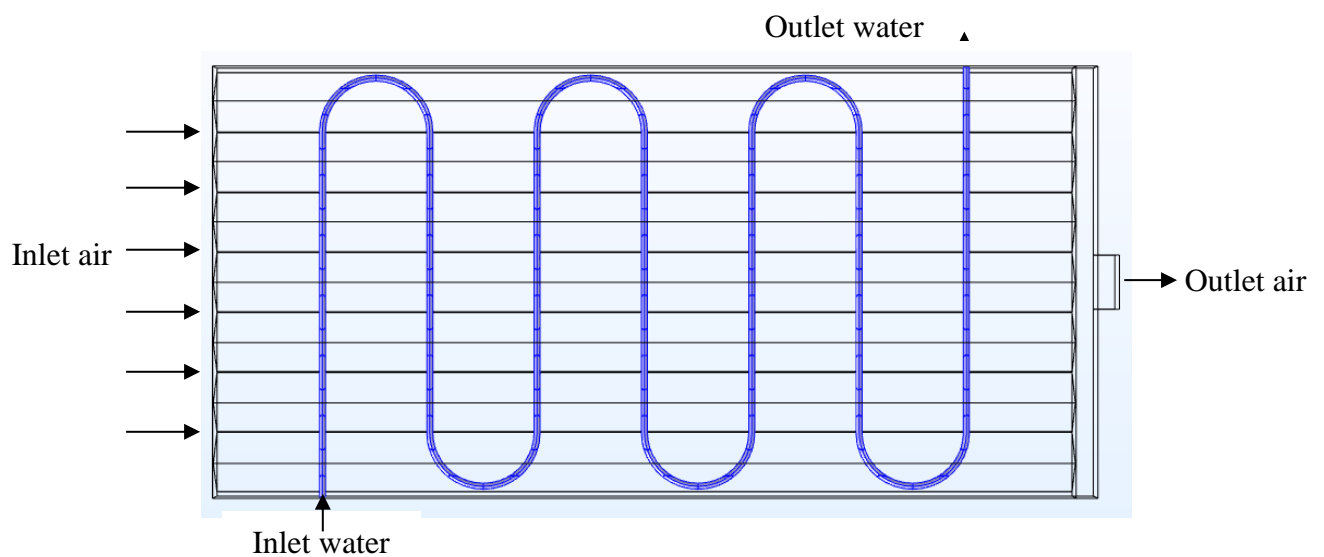


Fig. 4.2 Cross section of DPSC.

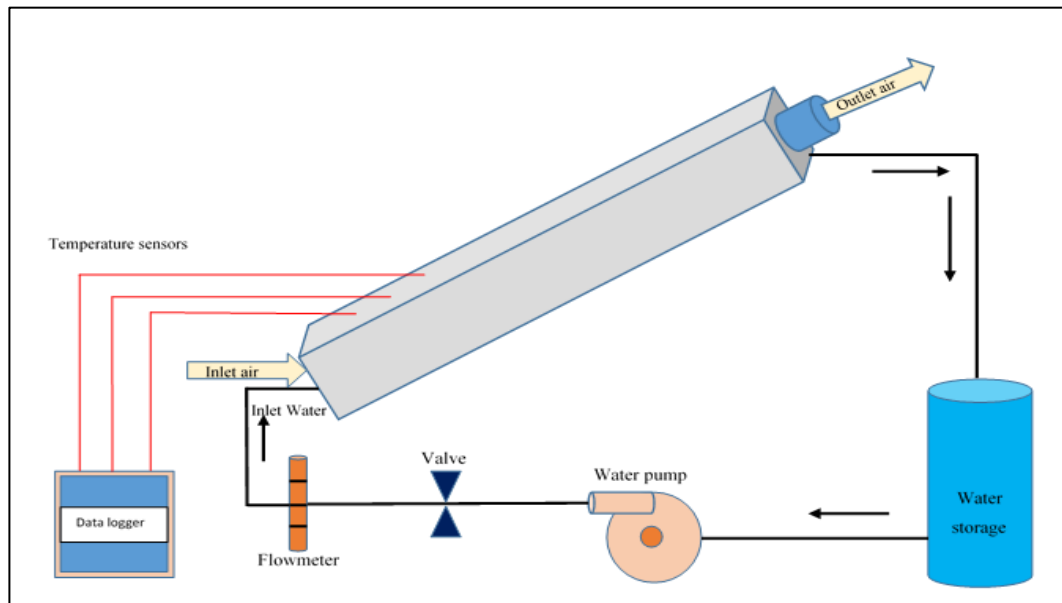


Fig. 4.3: Schematic of experimental rig.

a) Glass cover

Glass is commonly used to cover solar collectors as short-wave solar radiation can be absorbed high range from solar irradiance. The thickness of the glass used, is 3 mm and has very high transparency. The glass also isolates the absorption plate from the surrounding air, thereby reducing losses by convection heat transfer. Another function of the glass is to prevent dust from entering the absorption plate from the outer circumference.

b) Absorber Plate

The absorber is the essential element of the collector, protected by the bottom insulation with the top edges lined with glass. It converts the absorbed solar radiation through the glass cover into heat energy. Often the absorption plate is made of metal that has a high ability to absorb the largest amount of radiation and transferred to water pipes and air channels, such as aluminum. Absorber plate that used was corrugated with dimensions (2*1*0.1) m. It is painted with a black paint to improve absorption solar radiation. Figure 4.3 shows the absorber plate.

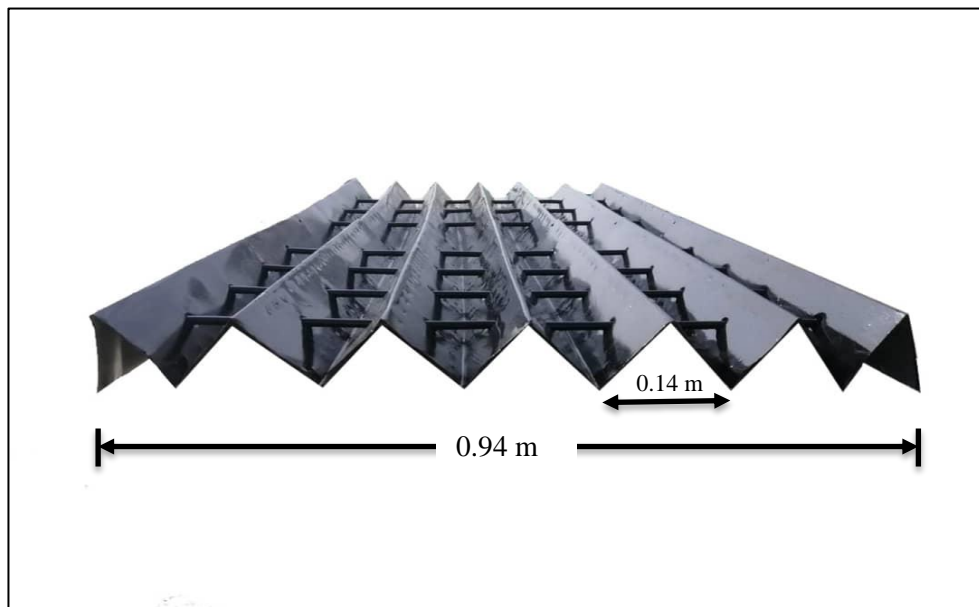


Fig. 4.4: Absorber plate.

c) Water pipe

The water pipe that use, is arranged in zig-zag shape. It is made from copper because it has high activity of heat transfer between absorber plate and water pipes. The absorption plate is perforated by transverse size of the tube diameter with small clearance to allow the pipeline to enter through it. Water pipe have two ports, input and output.

d) Insulation

The insulating material is mounted at the collector's back and sides. It decreases the losses from collector to surrounding. The thermal insulation that used is fiber glass with thermal conductivity of (\quad) .

e) Casing or Container

In order to keep the collector from dirt and moisture in a container. The container is made of wood with a thickness of 2.5 cm. The container is covered with glass wool insulation with thickness of 2 cm from all sides. Figure 4.4 showed the casing of collector.



Fig. 4.5: Casing.

Table 4.1 shows the specifications of the dual-purpose flat-plate solar collector.

Table 4-1: Specifications of dual purpose flat plate solar collector.

Specification	Details
Dimension of collector	(200x100x12) cm
Glass cover thickness	0.32 cm
Aluminum Absorber plate thickness	0.1 cm
Dimensions of triangles face in the absorber plate	(14x12x12) cm
Tilt angle	25°
Copper water pipe diameter	1cm
Space between the twisted pipes	25cm
Total water pipe length	750 cm
Glass wool insulation thickness	2.5 cm

4.2.2 Water pump

The electric water pump is located at the side of the system, between the water storage tank and the solar collector. Used to circulate the water from the water tank to the solar collector in closed system. Table 4.2 showed electric pump specifications.

Table 4-2: The specification of the water pump.

Data			N	Q max Lit/min	Power W
V	Hz	A			
220	50	0.75	2500 rpm	15	160

4.2.3 Fan

Air pull fan fixed on port of exit air to pull air through collector as clear in figure 4.5. Table 4.3 showed the specification of fan.

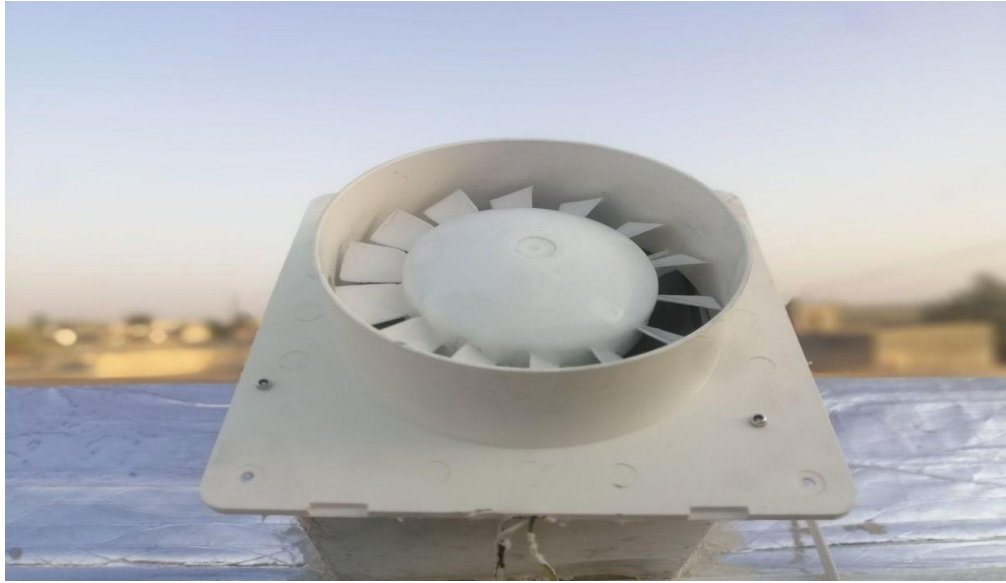


Fig. 4.6: Fan.

Table 4-3 :The specification of fan.

Data			N	Power W
V	Hz	A		
220-240	50	0.2	500 rpm	30

4.3 The measurement devices

In order to measure these parameters, measuring devices were used, which are described in detail below:

4.3.1 Data loggers

Two data logger with the specification as follows were used:

- ❖ 8-channel temperature data loggers V2 module HC-02.
- ❖ Its dimensions are 98mm×82mm×30mm.
- ❖ Can be controlled from a Computer by command control.
- ❖ Run on power supplied from USP source.

This device used to show the temperature value measured for each of the 8 attached sensors as Illustrated in figure (4.6). Temperature range to be

measured from (- 55 °C to 125 °C) with a max error ± 0.5 ° C. for these experiments, two devices were used.



Fig. 4.7: Data logger.

4.3.2 Temperature sensors

To measuring temperature at deferent places in the system, seventeen temperature sensors K type were used (fig. 4.7). This sensors connected to data logger to recording temperature reading. Sensors have been distributed as follows:

- Nine sensors fixed in air passage inside the collector.
- Two sensors fixed on the absorber plate surface.
- Two sensors at the inlet and outlet of the water.
- One sensor fixed on the glass surface.
- One sensor in port of outlet air.
- One sensor inside water storage tank.
- One sensor to measured ambient temperature.



Fig. 4.8: Temperature sensors.

4.3.3 Solar power meter

Protek model DM-301 shown in figure (4.8) was used to measure solar irradiance incidence, that device consists of the solar cell (solar panel) and an ohmmeter to measure solar cell DC voltage in m installed at 200 m volt-2000 m volt and converted to solar irradiance w / m^2 , calibration of the device shown in Appendix (A).



Fig. 4.9: Solar power meter.

4.3.4 Anemometer

Wind speed was measured with anemometer (HT-81). The measured range from 0.1 to 10 m/s, an error ± 0.1 . As clear in figure 4.9.



Fig. 4.10: Anemometer.

4.3.5 Water flow meter

Water flow meter is used in the water cycle to control the water flow rate through the collector. The flow meter is used for various ranges from 16 to 160 L/h an error $\pm 5\%$ as shown in figure 4.10.



Fig. 4.11: Water flow meter.

CHAPTER FIVE

RESULTS AND

DISCUSSION

CHAPTER FIVE

RESULTS AND DISCUSSION

5.1 Introduction

This chapter includes showed and analyzing the experimental and numerical results. Experiments were recorded in Al-Muthanna city, Iraq in (June and July), (2020). The study presents the effect of many parameters on the efficiency of DPSC system such as ambient temperature, water volumetric flow rate and solar radiation. All numerical results were performed by using COMSOL Multiphysics ver. 5.5 program.

5.2 Numerical simulation results

5.2.1 Validation of model

In order to verify accuracy of the numerical results that are achieved by using COMSOL program, the results were compared with previous study and present experimental results. A comparison between the experimental work of Omid et al. [12] with the present numerical work. Their results of Omid [12] for the DPSFC has specification as follow: dual purpose flat plat collector, the dimension of absorber plate was (1.94*0.94*0.01)m, inline water pipes with 0.7 cm diameter, air triangular fins was bolded below absorber plate with angle of 60°. The results of the comparison show that the present model of present work have enhancement in performance of dual purpose solar collector comparison with that of experimental works of Omid [12] as shown in figure 5.1.

Figure 5.1 shows the experimental results of the efficiency for Omid [12] and the results of present work. Noticed the results of present work improved the efficiency at rate of 2.4% comparison with previous work.

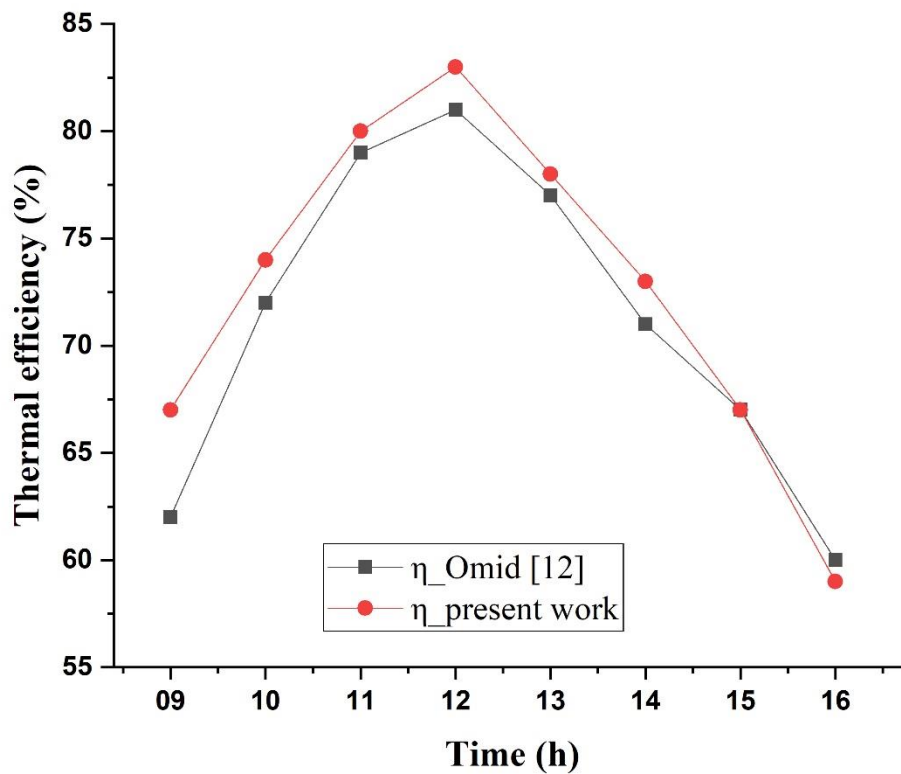


Fig. 5.1: Comparison between experimental results of Omid [12] with numerical results of present work of efficiency.

Notice: in all numerical results which studied the effect of ambient temperature, solar radiation, wind speed, inlet water temperature and water volume flow rate, the input data used in the simulation for (20/6/2020) obtained from experimental data for present work.

5.2.2 Effect of ambient temperature

The study of effect of variation ambient temperature on DPSC performance were carried out with the other parameters remain same at in each cases to find out real effect of ambient temperature only. The study includes five cases of ambient temperature (15, 25, 35, 45 and 55) $^{\circ}\text{C}$. The results show that the outlet water and air temperature increases with the

ambient temperature increases as shown on figure 5.2. The outlet water temperature was (64.44, 65.85, 67.38, 68.80 and 70.18) $^{\circ}\text{C}$ for cases with ambient temperature at (15, 25, 35, 45 and 55) $^{\circ}\text{C}$ respectively with increment rate of outlet water temperature (1.4) $^{\circ}\text{C}$ for every (10) $^{\circ}\text{C}$ ambient temperature increases with the other parameters remains constant. The outlet air temperature was (73, 79.6, 83.2, 88.5 and 90.1) $^{\circ}\text{C}$ for (15, 25, 35, 45 and 55) $^{\circ}\text{C}$ respectively.

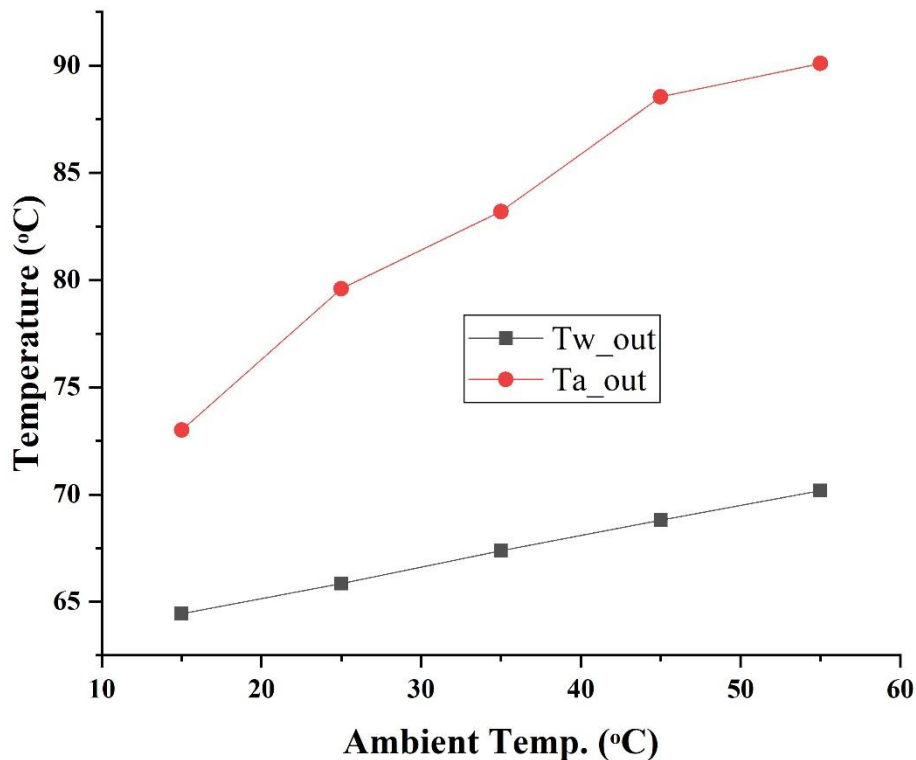


Fig. 5.2: Variation of outlet temperature with ambient temperature variation.

5.2.3 Effect of solar irradiance

Solar irradiance is a source of heat in solar collectors systems, the performance of this system depend mainly on it, so, the effect of variation of solar radiation was studied in this section. The effect of variation studied at (300, 500, 800 and 1100) W/m^2 with the other parameters ambient temperature, inlet water temperature, and outlet air speed are constant, as shown in figure 5.3. The outlet temperature increases with solar irradiance increases, it was (52.9, 56.64, 62.4 and 68.61) $^{\circ}\text{C}$ for (300, 500, 800 and 1100) W/m^2 respectively for water and (57.6, 65.89, 78.36 and 83.2) $^{\circ}\text{C}$ for (300, 500, 800 and 1100) W/m^2 respectively for air.

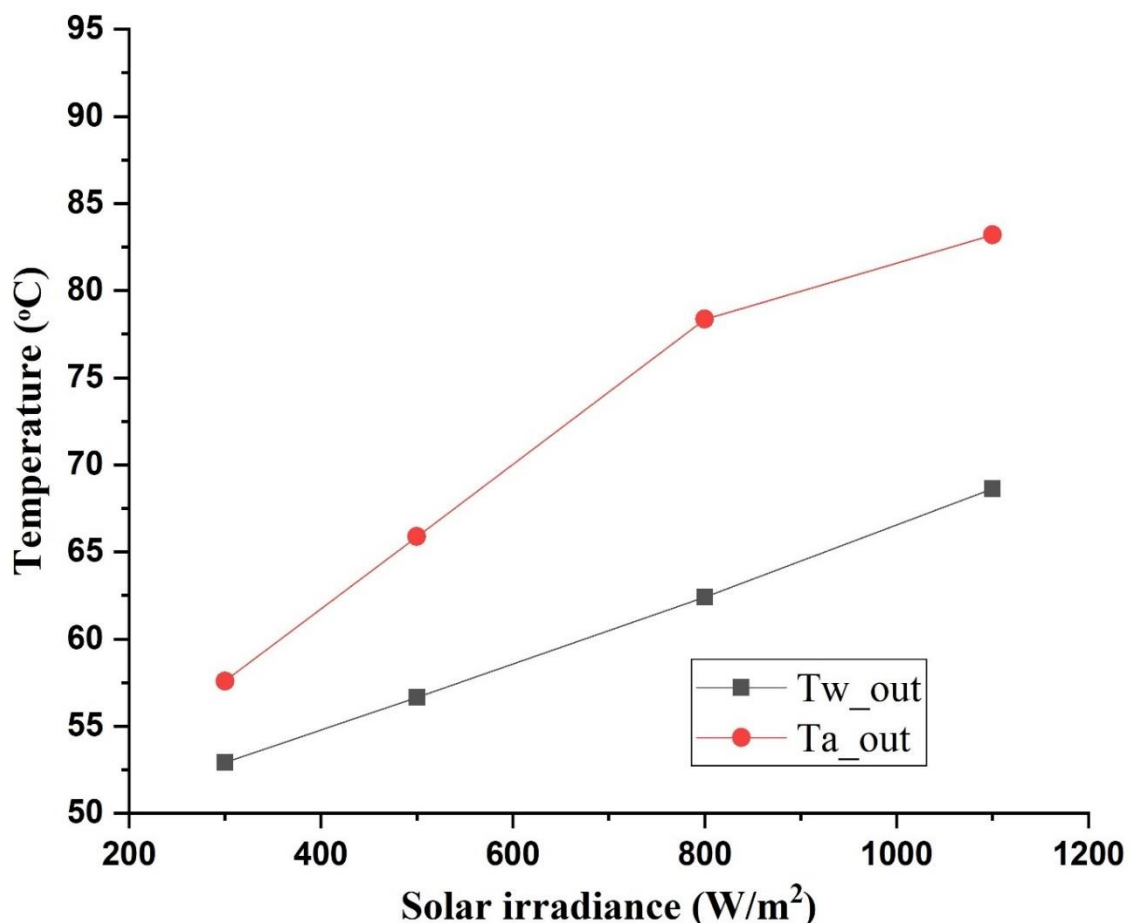


Fig. 5.3: Variation of outlet temperature with variation of solar irradiance.

5.2.4 Effect of outlet air velocity

The air was pulled from the upper collector by fan air to pull the air through inside the collector. The air velocity effect on rate of heat transfer between working fluid and absorption part. In this section, the variation of outlet air velocity was conducted at (0.5, 1, 1.5 and 2) m/s. figure 5.4 shows that the outlet temperature decreases with outlet air velocity increases. The results of outlet water temperature was (68.8, 65.55, 63.35 and 61.75) °C for (0.5, 1, 1.5 and 2) m/s respectively, and outlet air temperature was (84.4, 78.5, 73.5 and 69.04) °C for (0.5, 1, 1.5 and 2) m/s respectively.

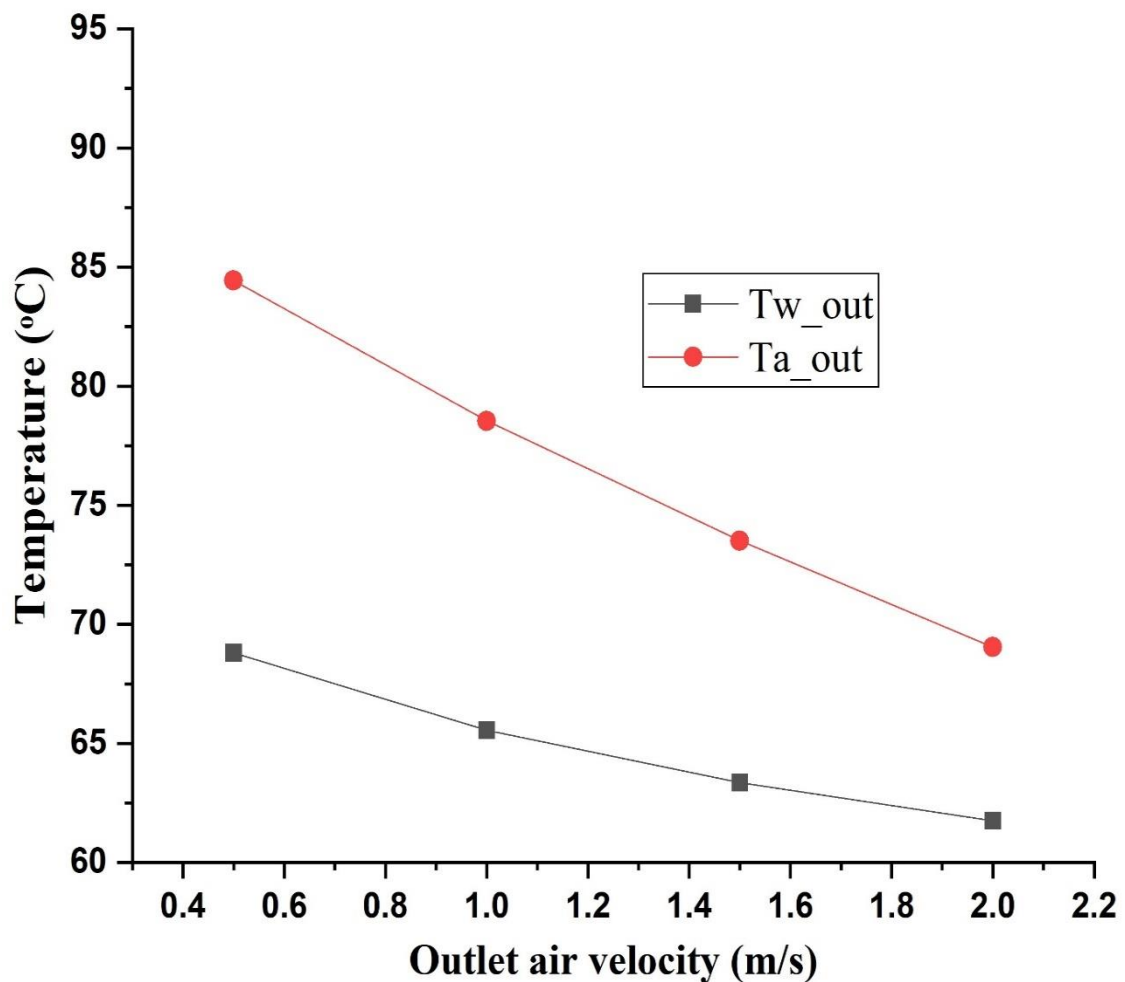


Fig. 5.4: Variation of outlet temperature with variation of outlet air velocity.

5.2.5 Effect of inlet water temperature

In closed solar collector systems, as this present work, the inlet water temperature increase gradually. In this study the effect of inlet water temperature was illustrated how it effected on performance of dual-purpose solar collector for four cases. Figure 5.5 shown that the outlet water temperature increases as inlet water temperature increases with high rate of solar radiation while the outlet water temperature was increase with solar radiation increase until a certain limit, then it will decreases due to low solar radiation rate, therefore, absorber plate temperature will decreases gradually and the heat will transfer from water to absorber surface and air flowing. The values of outlet water temperature was (46.93, 55.01, 65.55 and 71.29) °C for water, and (73.97, 76.78, 80.4 and 82.34) °C for air, for (25, 35, 45 and 55) °C inlet water temperature.

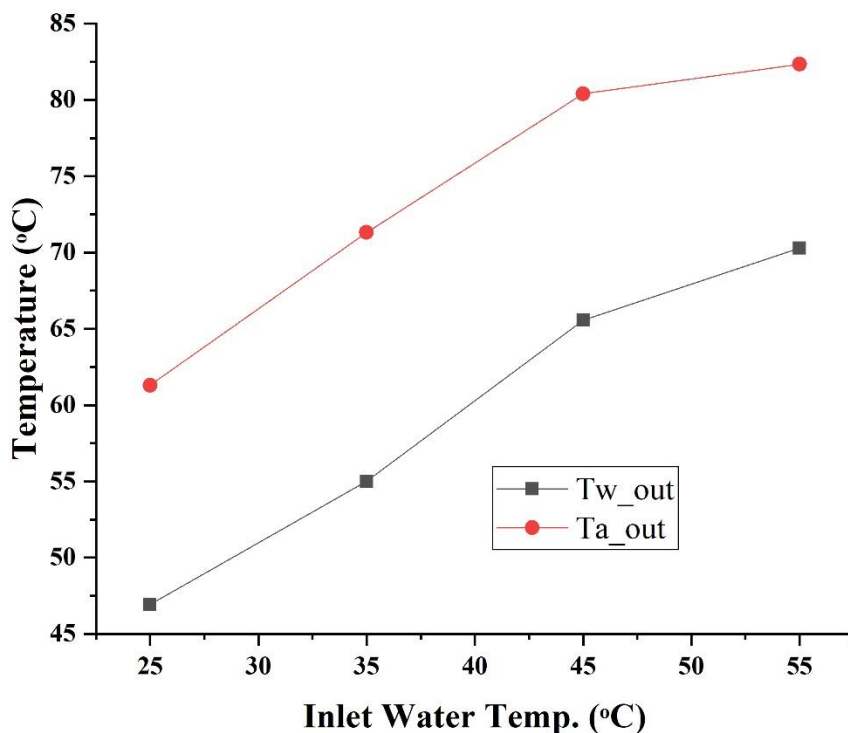


Fig. 5.5: Variation of outlet temperature with variation of inlet water temperature.

5.2.6 Effect of water volume flow rate

In this section, the effect of four different water volume flow rate was studied. The ranges were (40, 60, 80 and 100) L/h. the water volume flow rate is effecting directly on the heat transfer between water flowing and absorbaton part. Figure 5.6 shown that when the water volume flow rate increases the outlet temperature decreases. The values of outlet temperature was (76.62, 68.61, 64.211, 64) °C in water part and (88.1, 86.9, 84.8 and 84.7) °C in air part for (40, 60, 80, and 100) L/h respectively.

From above, it was illustrated that the variation in water part higher than variation in air part because the air don't effected mainly by volume flow rate change as water part. The temperature difference between maximum and minimum values of outlet temperature was (12.4 and 5.9) °C for water and air parts respectively.

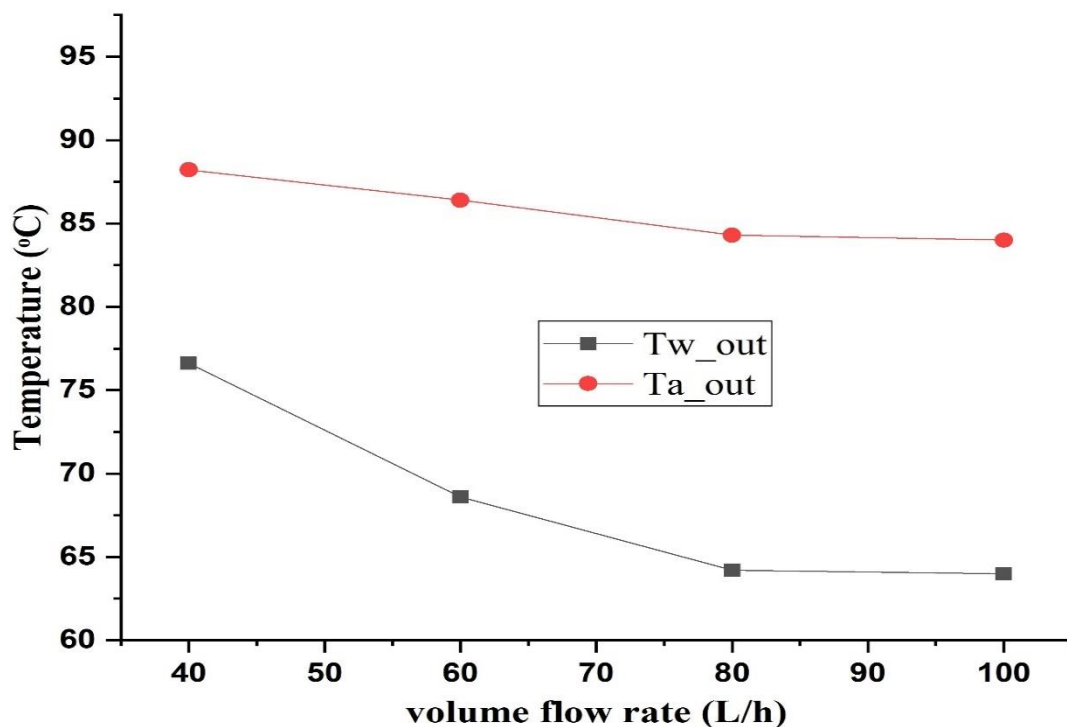


Fig. 5.6: Variation of outlet temperature with variation water volume flow rate.

5.2.7 Results of winter simulation days

After validated the accuracy of simulation model, winter days simulated in order to know the performance of dual purpose solar collector. The input data was taken from weather station in Engineering Technical College/Najaf. The water inlet temperature assumed constant in each hour simulation as well as open system. The time of run was start from 8:00 to 18:00 with step time 1 hour on 30/12/2019 and 18/2/2020.

Figures (5.7 to 5.9) shown the solar irradiance, ambient temperature and wind speed for both days of simulation.

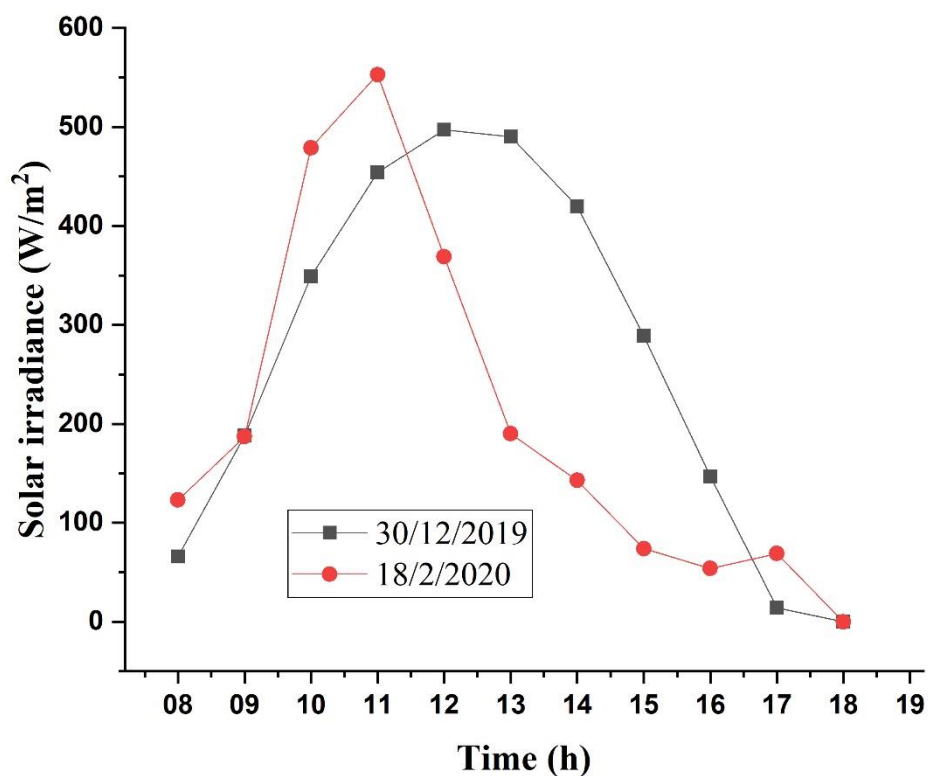


Fig. 5.7: Solar irradiance for simulation days.

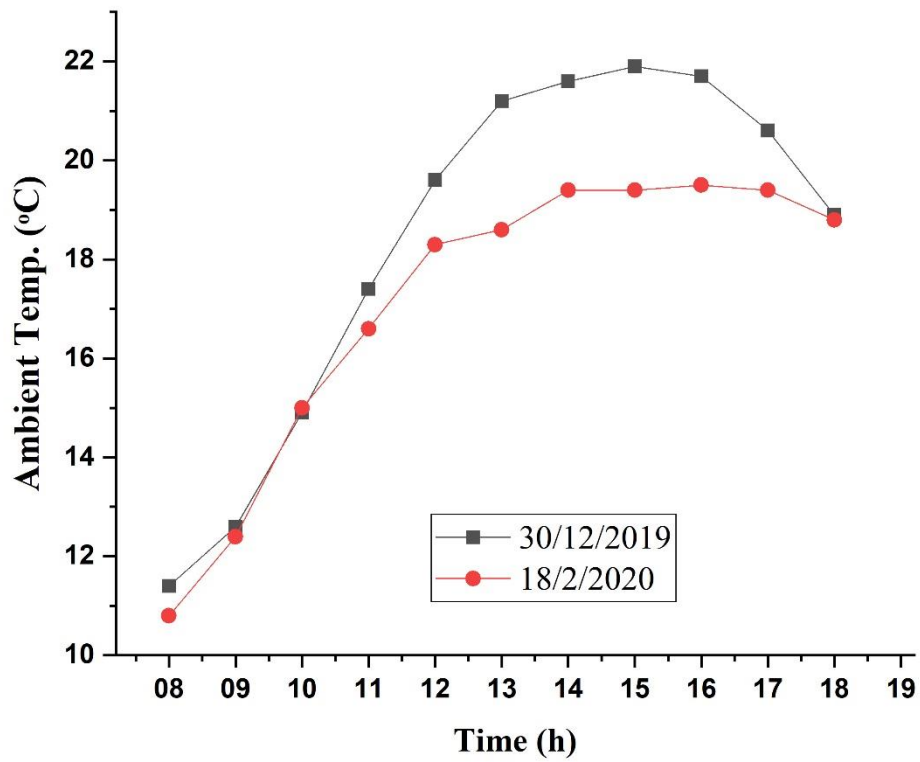


Fig. 5.9: Ambient temperature for simulation days.

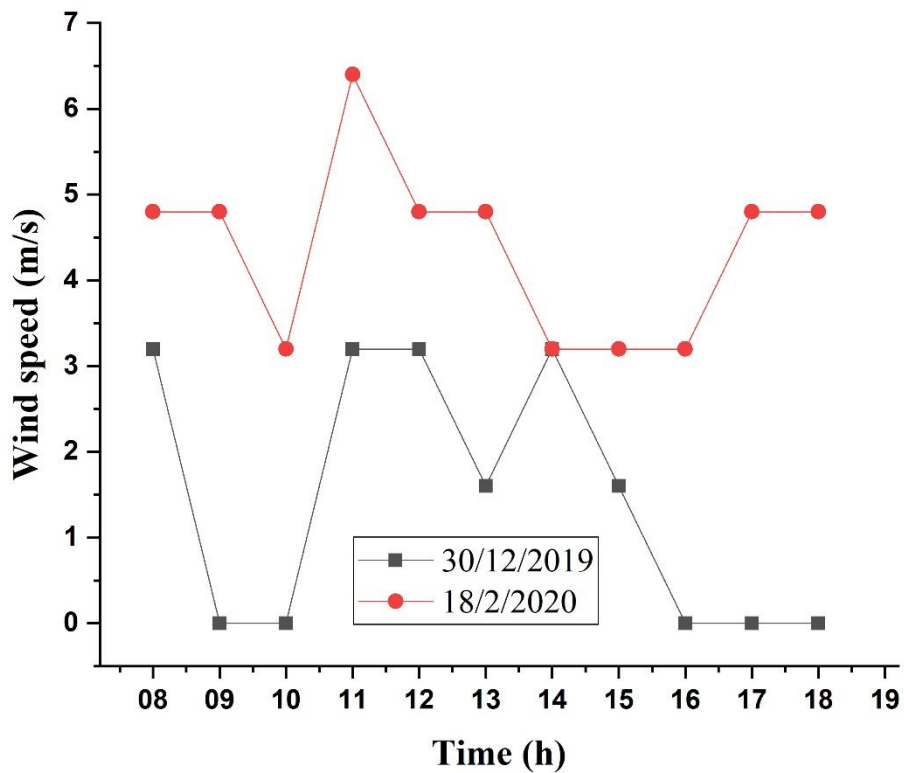


Fig. 5.8: Wind speed for simulation days.

Figures (5.10 & 5.11) showed that the outlet temperature for water and air parts with accepted rates of outlet temperature. The maximum outlet water temperature was 40.3 °C recorded on 18/2/2020 due to Haigh range of solar irradiance in this day. While the maximum outlet air temperature was 46.9 °C recorded on 30/12/2019.

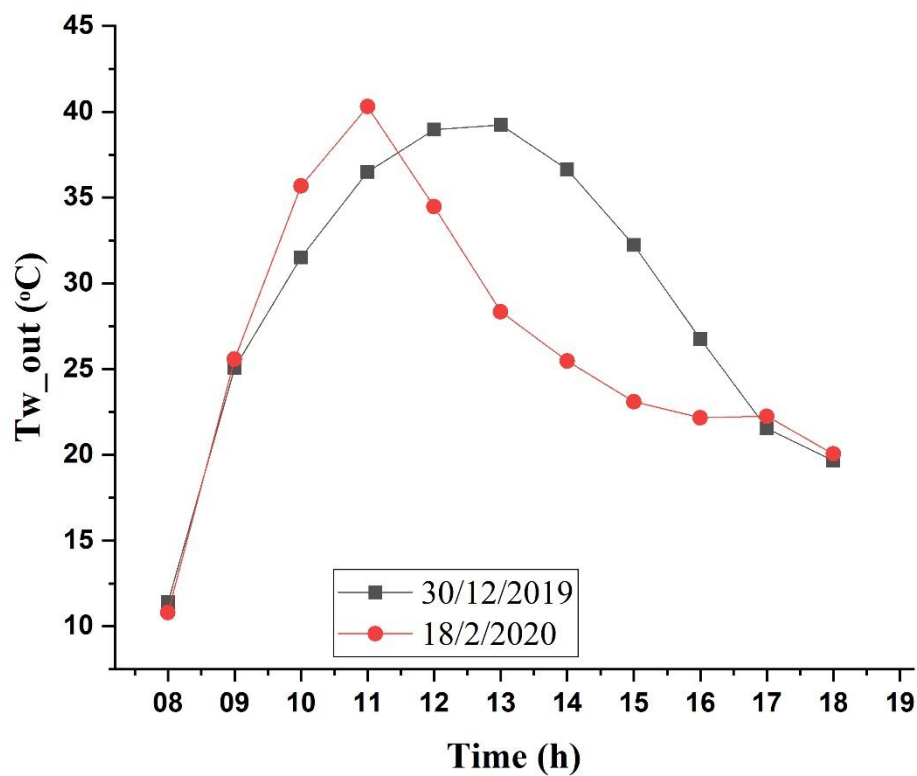


Fig. 5.10: Outlet water temperature for simulation days.

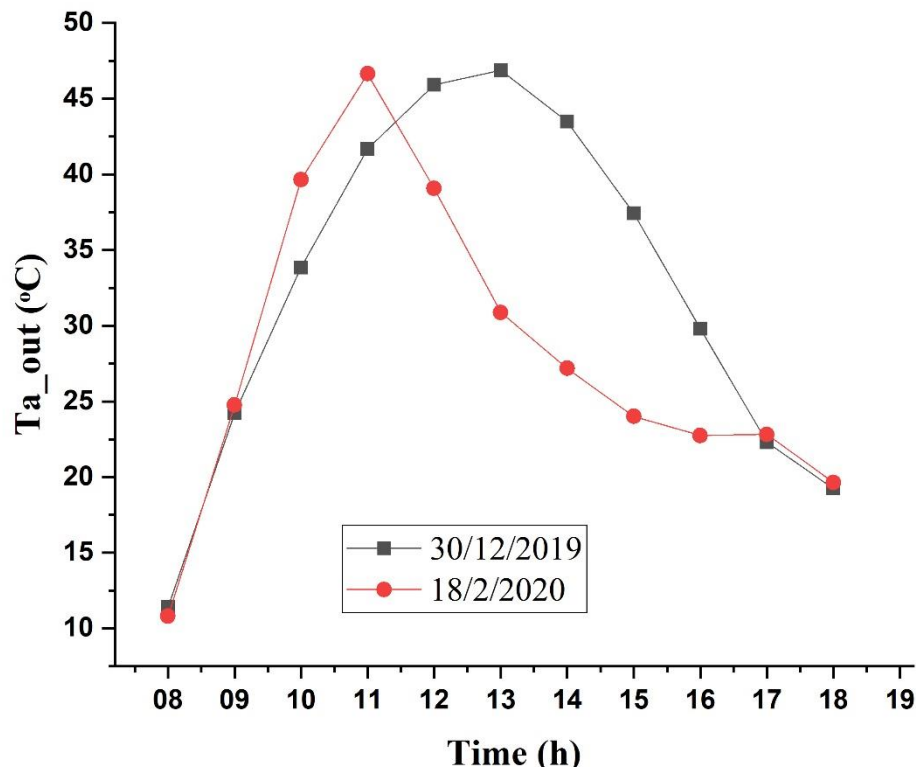


Fig. 5.11: Outlet air temperature for simulation days.

The maximum outlet air temperature recorded on 30/12/2019 although another day have higher rate of solar irradiance, but the ambient temperature for 30/12/2019 higher than 18/2/2020, whereas the outlet air temperature increase with the ambient temperature increase. Also the wind speed in 18/2/2020 higher than 30/12/2019 and the outlet air temperature decrease with wind speed increase.

5.2.8 Temperature distribution study

Figures (5.12 & 5.13) shown the temperature distribution inside the DPSC system included that: absorber plate surface, water pipes and air channel. The temperature distribution was at two days of experiments days, 19/6/2020 and 2/7/2020 at time (10:00, 12:00, 14:00 and 16:00) to clear who the heating distribution varying with the time.

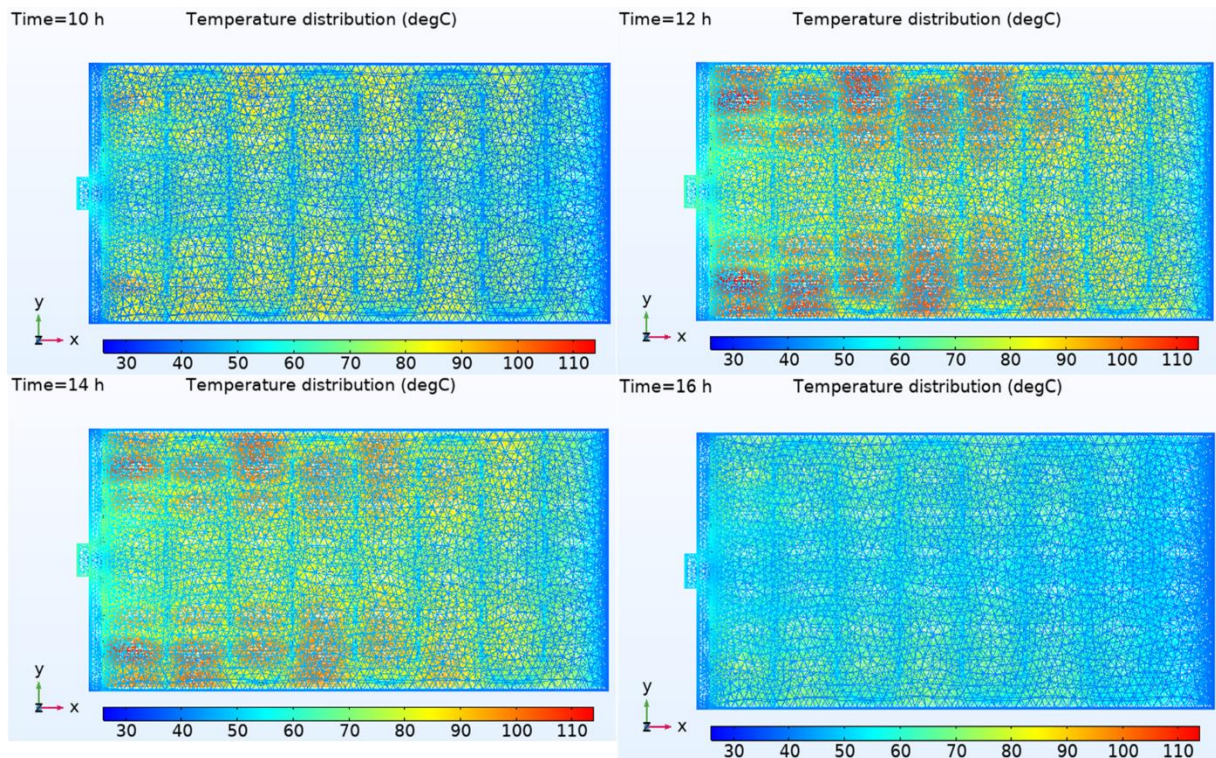


Fig. 5.12: Temperature contour 19/6/2020.

From above figure it is noticed that the maximum range of temperature at hour 12:00, and it increases gradually where the low rate at entering port and higher rate at the exit port, but the temperature decreases at center due to high air velocity that is product from the fan.

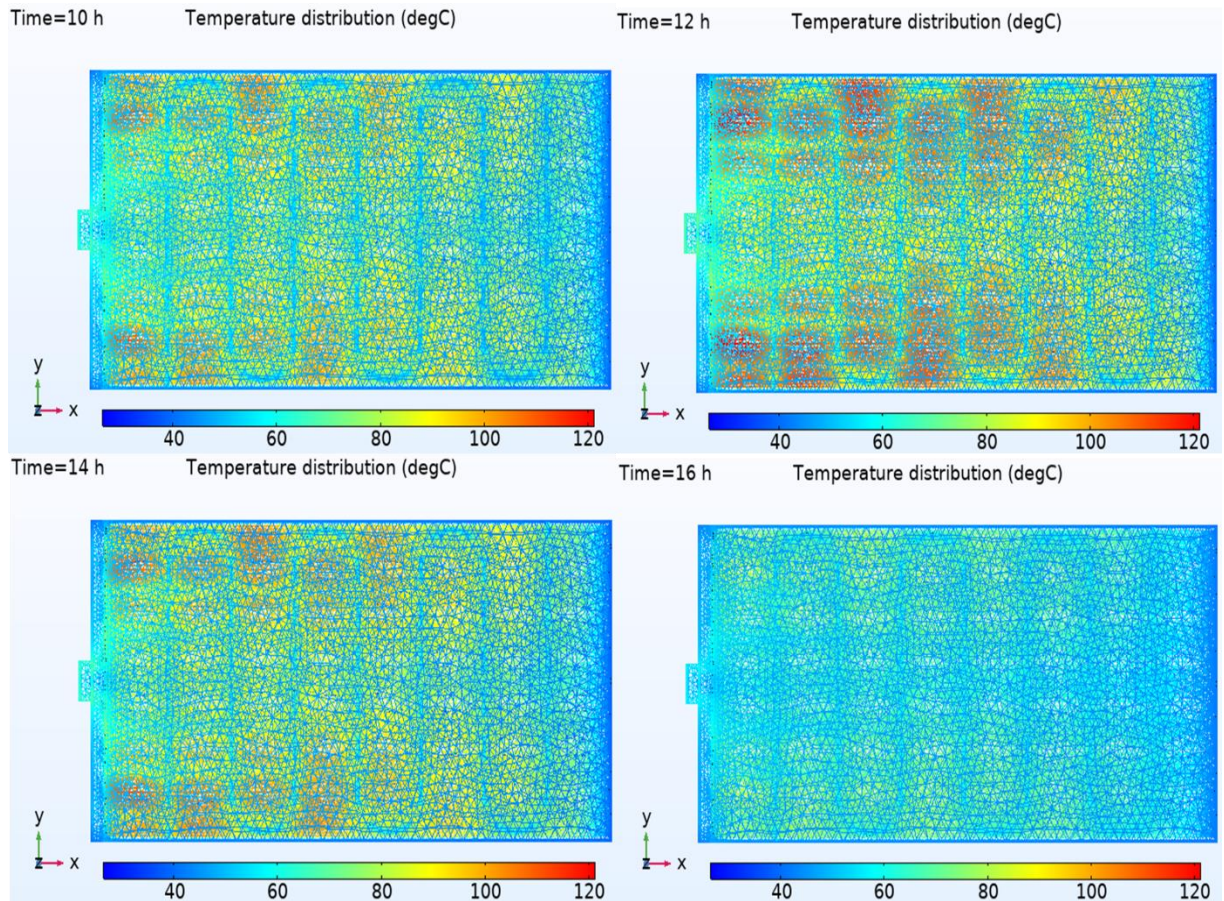


Fig. 5.13: Temperature contour 2/7/2020.

Figure 5.13 showing the temperature distribution for 2/7/2020 at four different time. The varying of distribution is same rate at figure 5.12 but in this day the average of temperature higher than previous section.

5.3 Experimental results

5.3.1 Comparison between experimental and numerical results of present work

Numerical study was carried out with the same weather conditions in which the experimental study conducted. Figures (5.14 to 5.17) clear a comparison between the experimental and numerical results of outlet water and air temperature for present work for two days at different water mass flow rate. Noticed a good agreement between experimental and numerical results.

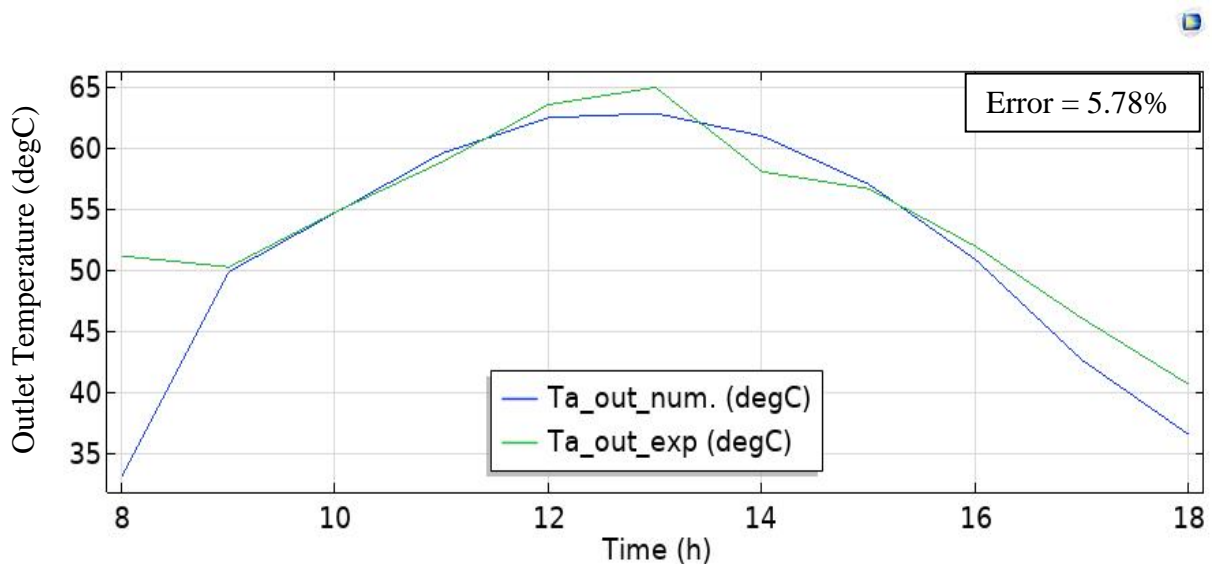


Fig. 5.14: Comparison between experimental and numerical results of present work of outlet air temperature, (19/6/2020).

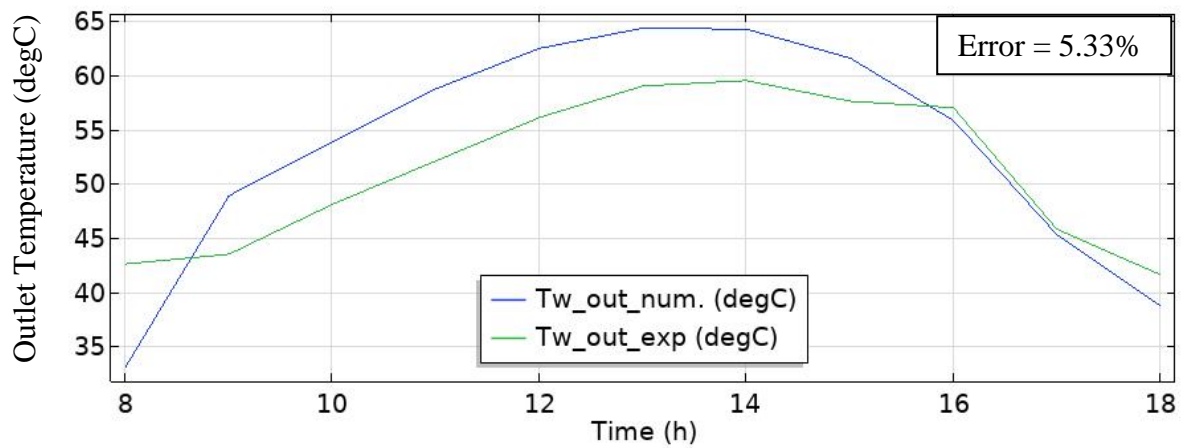


Fig. 5.15: Comparison between experimental and numerical results of present work of outlet water temperature, (19/6/2020).

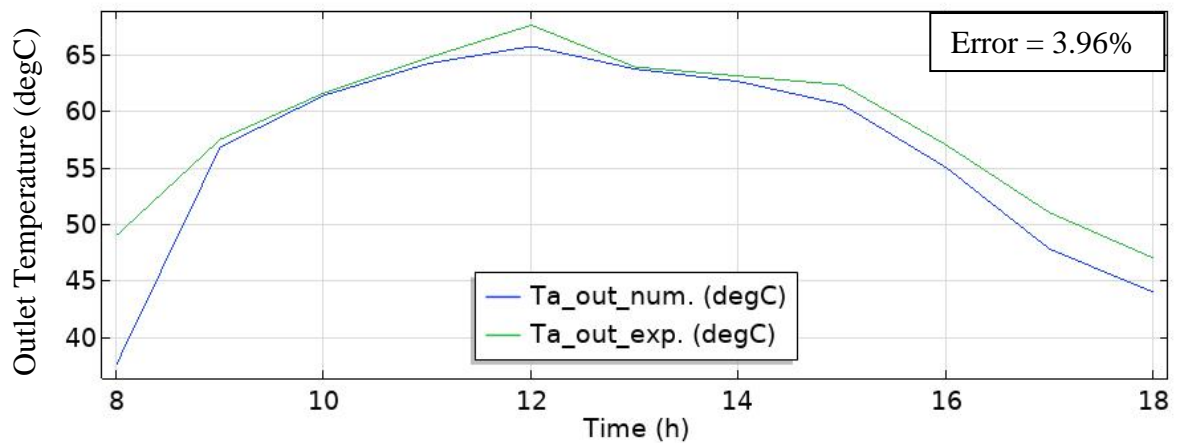


Fig. 5.16: Comparison between experimental and numerical results of present work of outlet air temperature, (2/7/2020).

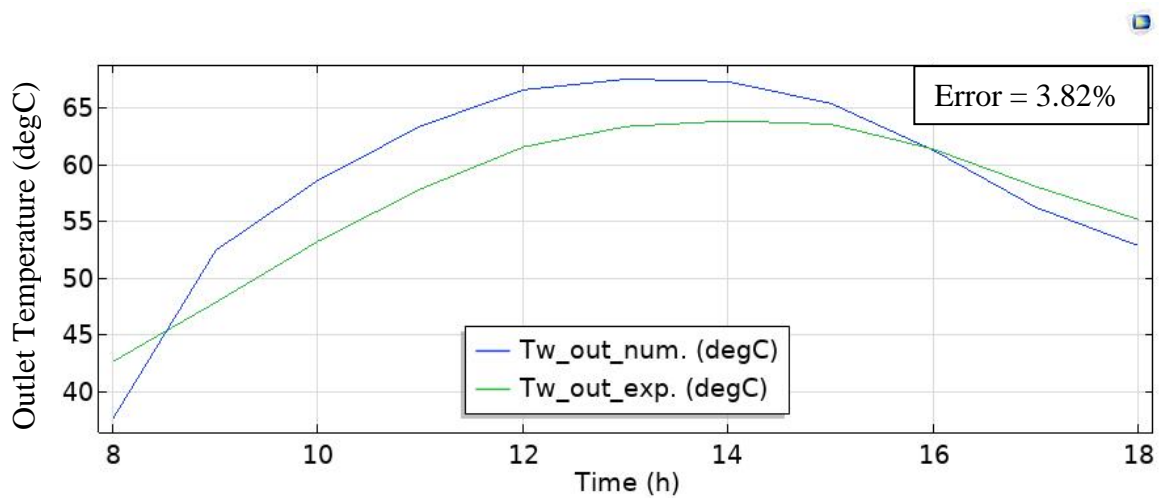


Fig. 5.17: comparison between experimental and numerical results of present work of outlet water temperature, (2/7/2020).

By using Root mean Square Error equation (RMSE) [46], the average error between experimental and numerical simulation results. The formula of RMSE equation is:

$$RMSE = \sqrt{\frac{1}{n} \sum_{i=1}^n (y_{num.} - y_{exp.})^2} \dots\dots\dots (5.1)$$

The average error was 4.72%.

5.3.2 The effect of weather condition

One of the aims of this study was studying the effect of the weather conditions on the performance of the DPSC, so, three different days were selected to carry out these study, which on 18-20/6/2020 at same volume flow rate, it which (60 l/h). The amount of solar radiation, wind speed and ambient temperature were measured by using devices calibrated each 15 minutes from 8:00 am to 6:00 pm at all experiments day. The solar meter fixed at the same tilt angle of collector slop to reading real amount of solar radiation that fell on the collector surface. Figures (5.18 to 5.20) Shows the solar radiation, ambient temperature and wind speed for each experiments days.

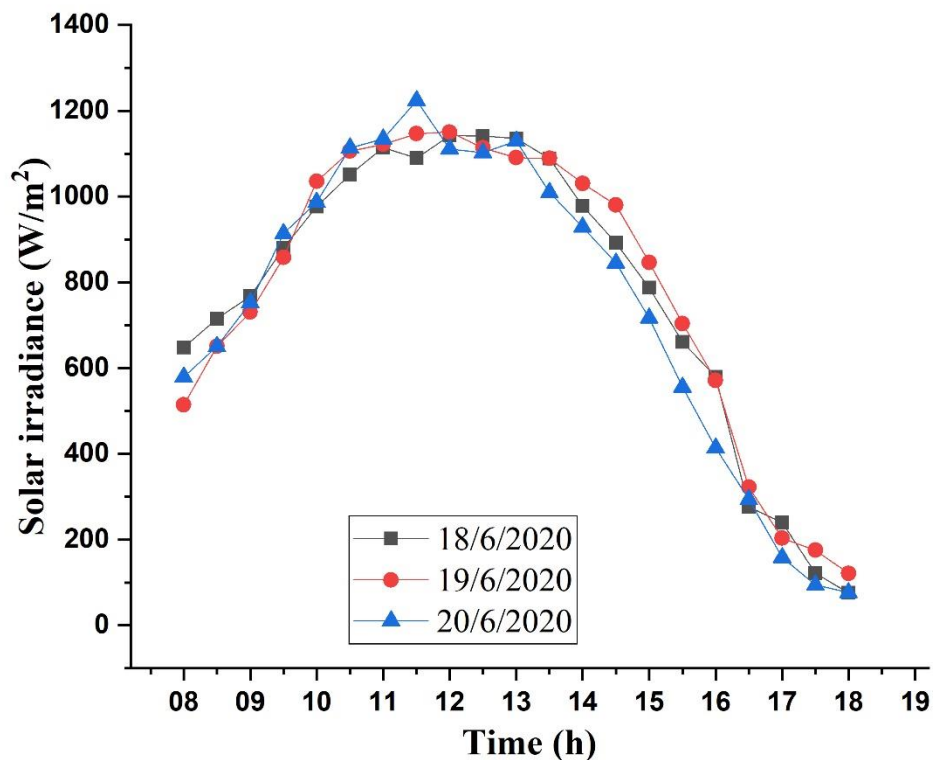


Fig. 5.18: Hourly variation in solar irradiance during testing days.

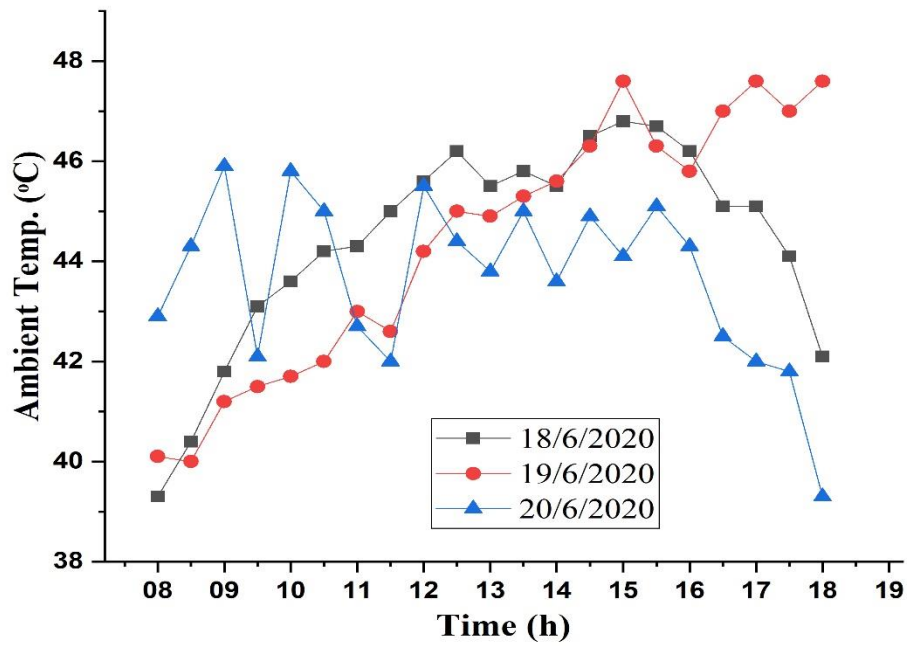


Fig. 5.20: Hourly variation in ambient temperature during testing days.

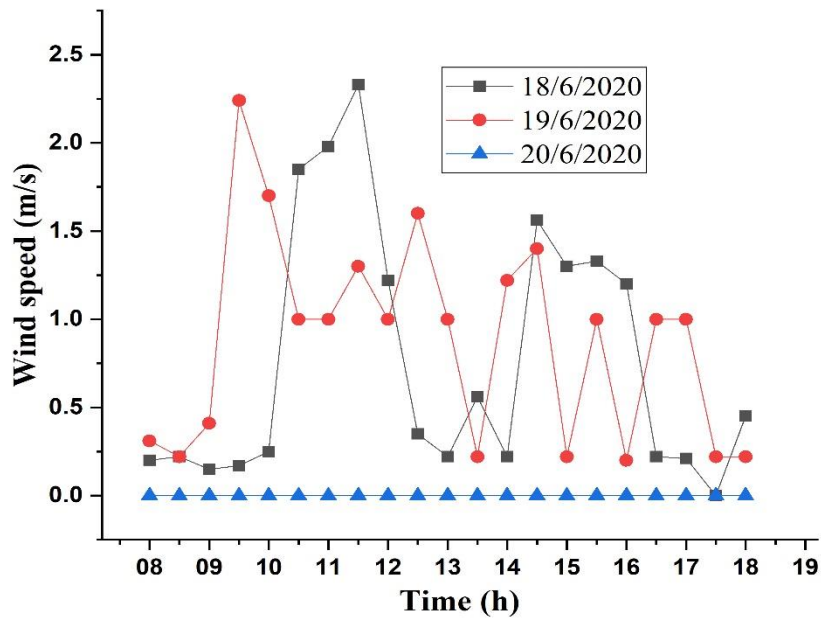


Fig. 5.19: Hourly variation in wind speed during testing days.

Figures 5.21 and 5.22 shows hourly variation of water and air outlet temperature during days of test. There is a remarkable increment in water outlet temperature rate on June 19, 2020 comparison with others days because this day have higher average of solar radiation, while the T_{w_out} in June 18, 20, 2020 was convergence approximately due to convergence the average of solar radiation. The maximum values of T_{w_out} for three tested days was 66.8 °C, 69.9 °C and 65.6 °C respectively on June 18, 19, 20, 2020. At the other side, the Air outlet temperature also variation with same average of T_{w_out} and the highest T_{a_out} recorded on June 19, 2020. The maximum values of T_{a_out} was 76.3 °C, 79.2 °C and 77.1 °C for June 18, 19 and 20, 2020 respectively.

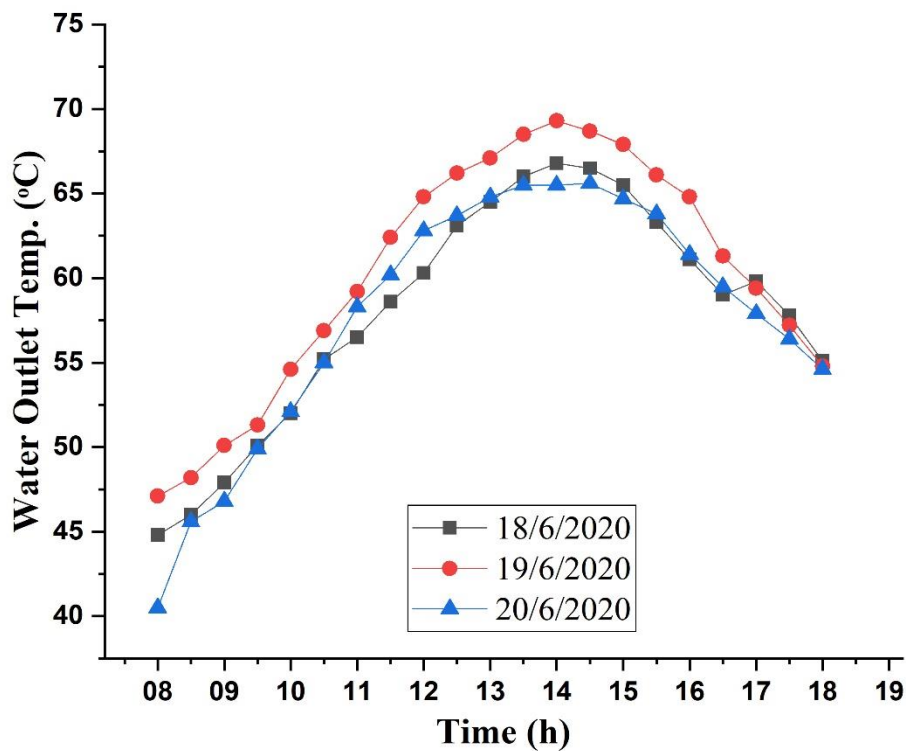


Fig. 5.21: Hourly variation of water outlet temperature during testing days.

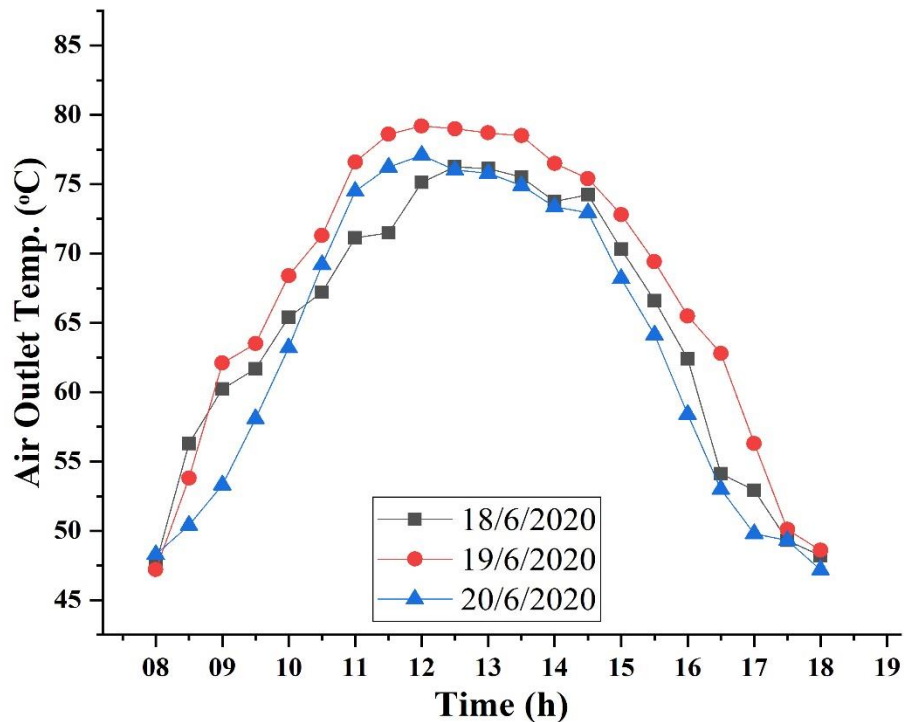


Fig. 5.22: Hourly variation of air outlet temperature during testing days.

Figure 5.23 and 5.24 shown the daily variation of useful heat that calculated for water and air parts for testing days. The useful heat is amount of heat using to heating working fluid in each DPSC parts. The variation rate depends on solar radiation falling on the absorbent part. The highest values of useful energy for water parts was 773.3 W, 933.2 W and 788.2 W on June 18, 19 and 20, 2020 respectively, and for air part was 584.6 W, 706.5 W and 621.3W on 18, 19 and 20 respectively. This values illustrated the effect of solar radiation on the useful heat, it increases with solar radiation increases.

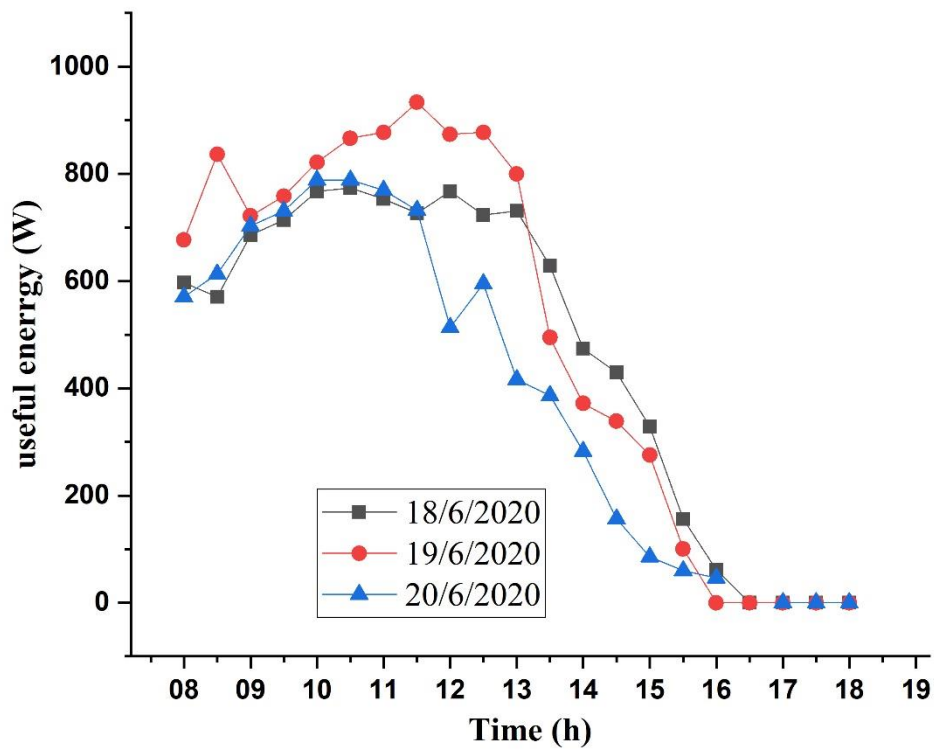


Fig. 5.24: Hourly variation of useful energy for water part for testing days.

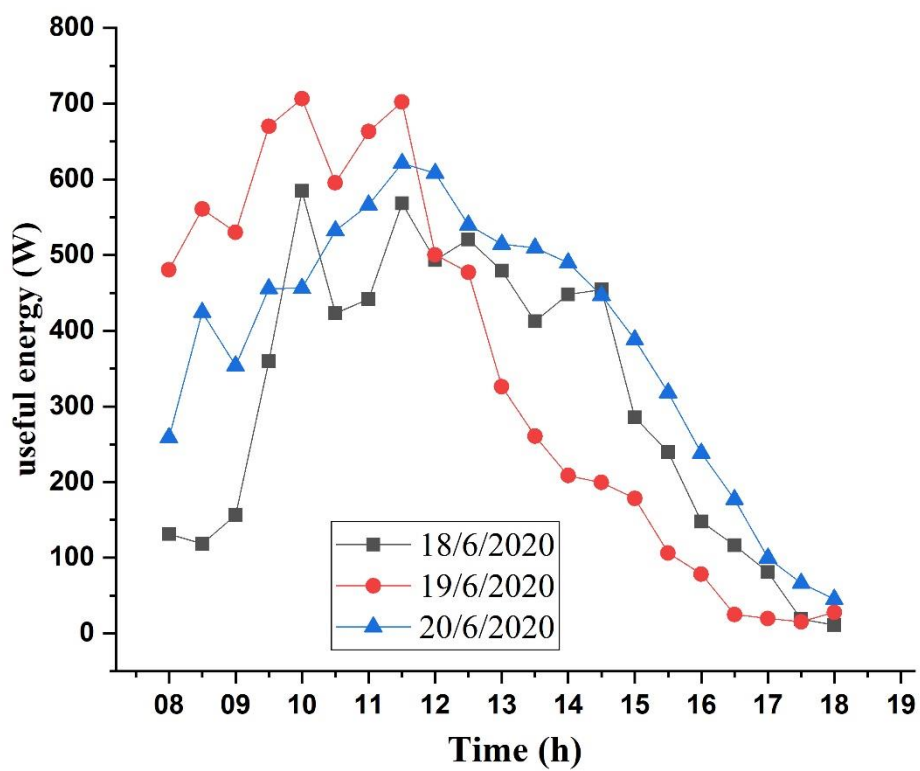


Fig. 5.23: Hourly variation of useful energy for air part for testing days.

Figure 5.25 clear the hourly variation of the thermal efficiency of DPSC for different testing days. The efficiency was calculated for June 18, 19 and 20, 2020. The maximum values of efficiency was 77.3%, 78%, 76.7% on June 18, 19 and 20, 2020 respectively.

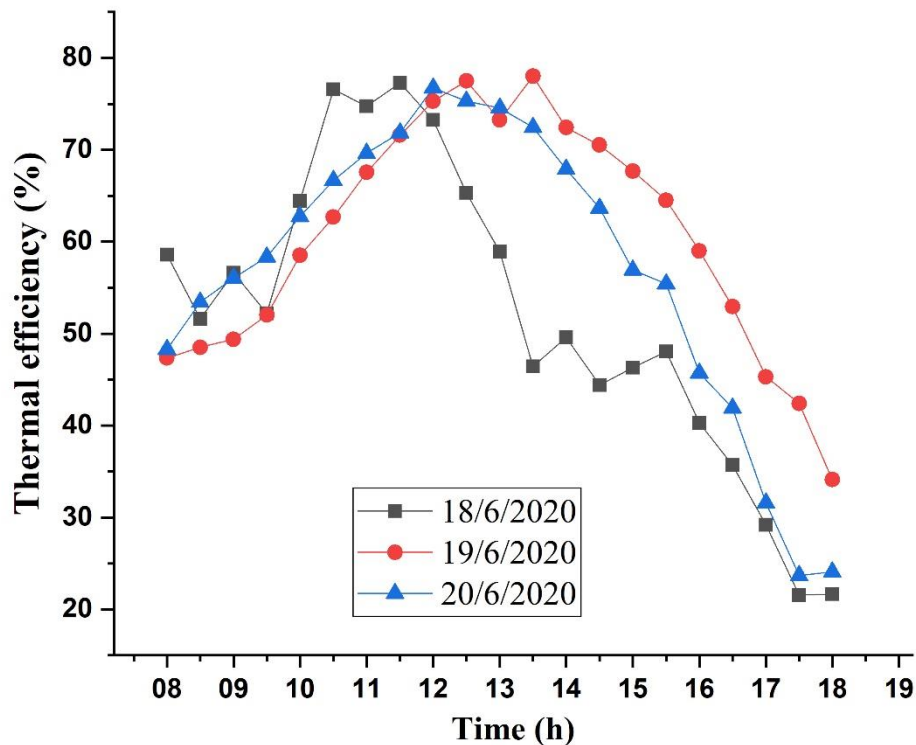


Fig. 5.25: Hourly variation of efficiency for testing days.

The maximum value of efficiency recorded on June 19, 2020 because that this day have higher value of useful energy. The testing days recorded convergence amount of solar radiation and useful energy with low increment on June 19. The average of efficiency of test days with water volume flow rate (60l/h) was 52.02%, 60.49% and 57% on June 18, 19 and 20, 2020 respectively.

5.3.3 Temperature differences results

The difference rate of water and air temperature is depend on the flow rate of working fluid to allowable the heat transfer from absorber plate to working fluid beside to another parameters. Figure 5.26 shows that temperature difference between entrances and excite water at different water volume flow rate (40, 60 and 80) l/h, on consecutive days to keep same weather conditions approximately. It is noticed from figure 5.26 clearly that the maximum water temperature difference can get with water volume flow rate (40 l/h) in duration from (10:00 to 11:30), it was (3.7 °C). The air temperature difference was studied at (0.5, 1 and 1.5) m/s air velocity at same water volume flow rate. Figure 5.27 shows that the maximum difference was (17.8 °C) for 0.5 m/s.

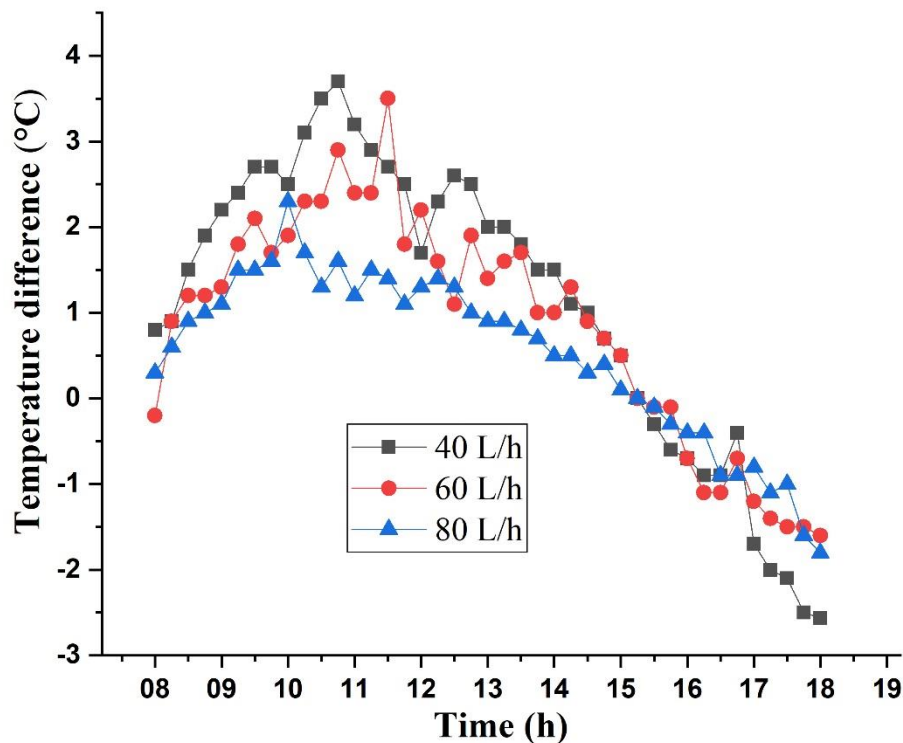


Fig. 5.26: Water temperature difference.

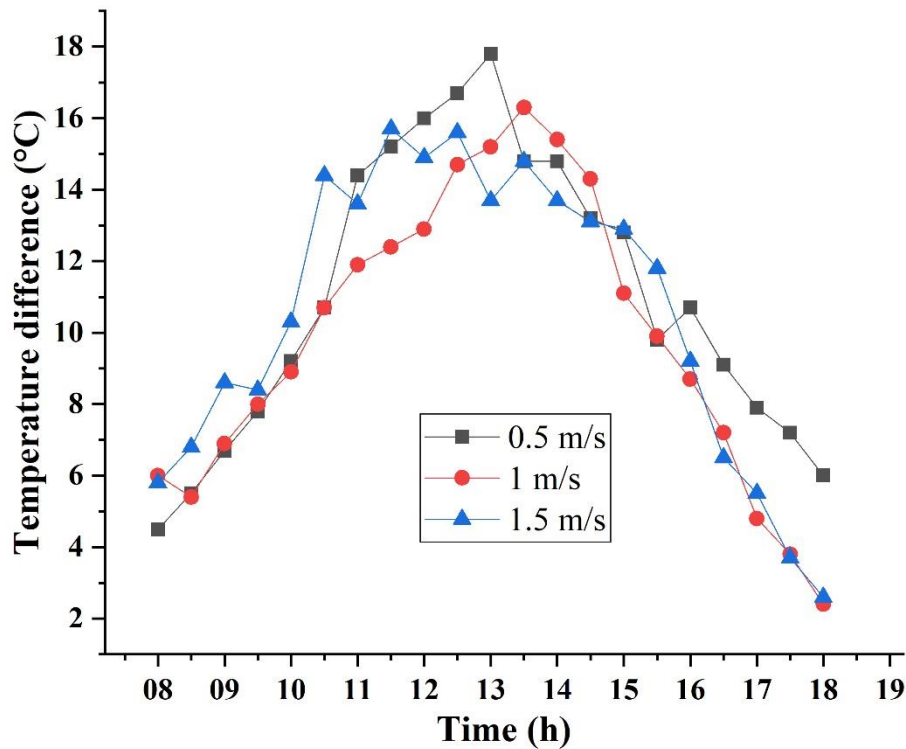


Fig. 5.27: Air temperature difference.

5.3.4 The efficiency of collector

Figure 5.28 clear that the hourly efficiency of (40, 60 and 80) L/h volume flow rate that was studied at time interval from (8:00 to 18:00) with convergent weather conditions. The total efficiency of collector was produced from summing water and air parts efficiency. The maximum efficiency recorded with (40 L/h) volume flow rate with convergence with the efficiency of other range of volume flow rate The maximum values of efficiency recorded was (83.3, 80.4 and 78.5) % for (40, 60 and 80) L/h respectively. The total average of DPSC efficiency was (53.35, 49.71 and 47.4) % for (40, 60 and 80) L/h respectively by using equation (3-8).

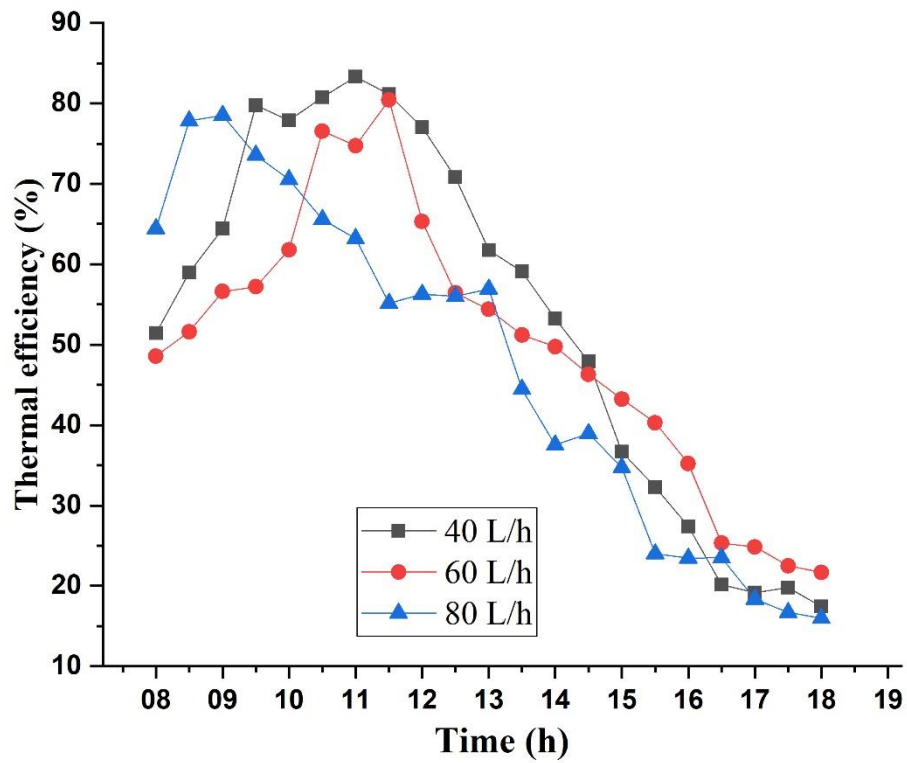


Fig. 5.28: Hourly efficiency of DPSC.

CHAPTER SIX

CONCLUSION AND

RECOMMENDATIONS

CHAPTER SIX

CONCLUSION AND RECOMMENDATIONS

The aim of this research is to studying the effect of solar radiation, ambient temperature, outlet air velocity, volumetric flow rate and inlet water temperature on the performance of dual purpose solar collector with new design of absorber plate. The study include numerical and experimental analyses with different volumetric flow rate (40, 60 and 80) L/h. numerical simulation was done by using COMSOL Multiphysics software program ver.5.5. In this chapter, the conclusions and recommendations was illustrated.

6.1 The conclusion

The following topics were conducted from this study:

- 1- A good agreement has been achieved between experimental and simulation results, it was 4.6% of mean error.
- 2- The outlet temperature (water and air) increases as the ambient temperature rise. The outlet water and air temperature have been recorded (64.44, 65.85, 67.38, 68.80 and 70.18)^oC and (73, 79.60, 83.2, 88.5 and 90.1) ^oC for ambient temperature (15, 25, 35, 45 and 55)^oC respectively.
- 3- The DPSFC evaluation of the effects of air velocity on the collector efficiency was included; they were tested at four variable air velocity (0.5, 1, 1.5 and 2) m/s.
- 4- The outlet temperature decreases with outlet air velocity increases. The results of outlet water temperature was (68.8, 65.55, 63.35 and 61.75) ^oC for (0.5, 1, 1.5 and 2) m/s respectively, and outlet air temperature was (84.4, 78.5, 73.5 and 69.04) ^oC for (0.5, 1, 1.5 and 2) m/s respectively.
- 5- There was interest in observing the effect of water volume flow rate, when the volume flow rate of water increases (40, 60, 80, and 100) L/h,

the outlet temperature decreases. The water outlet temperatures were (76.62, 68.61, 64.211, 64) °C and air outlet temperatures were (88.1, 86.9, 84.8 and 84.7) °C respectively.

- 6- The experimental and simulated results show that maximum efficiency can be achieved with 40 L/h volume flow rate of water. The maximum values of efficiency recorded was (83.3, 80.4 and 78.5) % for (40, 60 and 80) L/h respectively.

6.2 The recommendations

After this study, the authors have recommendations for the future work:

- 1- Study the different effect of weather conditions with new design of absorber plate.
- 2- For more efficient from solar radiation, tracing system, concentrating system and multi-layer glass cover can uses.
- 3- Studying the effect of add obstacles in air passage to increases the effectiveness of heat transfer.

REFERENCES

REFERENCES

- [1] F. Chabane and E. Sekseff, “Experimental Study of a Double Glazed Solar Air Collector,” *Iran. J. Energy Environ.*, vol. 9, No. 3, pp. 163–167, 2018.
- [2] N. K. M. A. Alrikabi, “Renewable Energy Types,” *J. Clean Energy Technol.*, vol. 2, No. 1, pp. 61–64, 2014.
- [3] John A. Duffi and William A. Beckman, *Solar Engineering of Thermal Processes*, No. 4. 2013.
- [4] Soteris A. Kalogirou, *Solar Energy Engineering Processes and Systems*. Second Edition, ISBN–13: 978-0-12-397270-5 ,USA, 2014.
- [5] L. Szabó, “The history of using solar energy,” in *The 7th International Conference on Modern Power Systems(MPS 2017) Romania*, 2017, p. 8.
- [6] J. Fan, Q. Huang, D. M. Sumner, and D. Wang, “A simple method for partitioning total solar radiation into diffuse/direct components in the United States,” *Int. J. Green Energy*, vol. 15, No. 9, pp. 497–506, 2018.
- [7] <https://globalsolaratlas.info/map> .
- [8] C. C. Newton, “A Concentrated Solar Thermal Energy System”, Department of Mechanical Engineering, FAMU-FSU COLLEGE OF ENGINEERING, THE FLORIDA STATE UNIVERSITY, USA, 2007.
- [9] A. T. Mustafa, H. H. Al-Kayiem, and S. I. U. Gilani, “Investigation and evaluation of the solar air collector model to support the solar vortex engine,” *ARPJ Journal of Engineering and Applied Sciences*, vol. 10, No. 12. pp. 5309–5319, 2015.
- [10] M. R. Assari, H. B. Tabrizi, and I. Jafari, “Experimental and theoretical investigation of dual purpose solar collector,” *Sol. Energy*, vol. 85, No. 3,

- pp. 601–608, 2011.
- [11] J. Ma, W. Sun, J. Ji, Y. Zhang, A. Zhang, and W. Fan, “Experimental and theoretical study of the efficiency of a dual-function solar collector,” *Appl. Therm. Eng.*, vol. 31, No. 10, pp. 1751–1756, 2011.
- [12] O. Nematollahi, P. Alamdari, and M. R. Assari, “Experimental investigation of a dual purpose solar heating system,” *Energy Convers. Manag.*, vol. 78, pp. 359–366, 2014.
- [13] K. Pottler, C. M. Sippel, A. Beck, and J. Fricke, “Optimized finned absorber geometries for solar air heating collectors,” in *Solar Energy*, 2000, vol. 67, No. 1–3, pp. 35–52.
- [14] P. Naphon, “Effect of porous media on the performance of the double-pass flat plate solar air heater,” *Int. Commun. Heat Mass Transf.*, vol. 32, No. 1–2, pp. 140–150, 2005.
- [15] M. A. Karim and M. N. A. Hawlader, “Performance evaluation of a v-groove solar air collector for drying applications,” *Appl. Therm. Eng.*, vol. 26, No. 1, pp. 121–130, 2006.
- [16] H. Esen, “Experimental energy and exergy analysis of a double-flow solar air heater having different obstacles on absorber plates,” *Building and Environment*, vol. 43, No. 6. pp. 1046–1054, 2008.
- [17] M. Mohanraj and P. Chandrasekar, “Performance of a forced convection solar drier integrated with gravel as heat storage material,” *Proceedings of the IASTED International Conference on Solar Energy, SOE 2009*. pp. 51–54, 2009.
- [18] E. K. Akpınar and F. Koçyiğit, “Energy and exergy analysis of a new flat-plate solar air heater having different obstacles on absorber plates,” *Appl. Energy*, vol. 87, No. 11, pp. 3438–3450, 2010.

- [19] K. Aoucs, N. Moumami, M. Zellouf, and A. Benchabane, “Thermal performance improvement of solar air flat plate collector: A theoretical analysis and an experimental study in Biskra, Algeria,” *Int. J. Ambient Energy*, vol. 32, No. 2, pp. 95–102, 2011.
- [20] V. V. Tyagi, A. K. Pandey, G. Giridhar, B. Bandyopadhyay, S. R. Park, and S. K. Tyagi, “Comparative study based on exergy analysis of solar air heater collector using thermal energy storage,” *Int. J. Energy Res.*, vol. 36, pp. 724–736, 2012.
- [21] S. M. González, S. F. Larsen, A. Hernández, and G. Lesino, “Thermal evaluation and modeling of a double-pass solar collector for air heating,” *Energy Procedia*, vol. 57, pp. 2275–2284, 2014.
- [22] W. Chang *et al.*, “The Theoretical and Experimental Research on Thermal Performance of Solar Air Collector with Finned Absorber,” *Energy Procedia*, vol. 70, No. Ming Li, pp. 13–22, 2015.
- [23] C. Sun, Y. Liu, C. Duan, Y. Zheng, H. Chang, and S. Shu, “A mathematical model to investigate on the thermal performance of a flat plate solar air collector and its experimental verification,” *Energy Convers. Manag.*, vol. 115, pp. 43–51, 2016.
- [24] A. A. Razak *et al.*, “Review on matrix thermal absorber designs for solar air collector,” *Renew. Sustain. Energy Rev.*, vol. 64, pp. 682–693, 2016.
- [25] A. Daliran and Y. Ajabshirchi, “Theoretical and experimental research on effect of fins attachment on operating parameters and thermal efficiency of solar air collector,” *Inf. Process. Agric.*, vol. 5, No. 4, pp. 411–421, 2018.
- [26] A. Fudholi and K. Sopian, “A review of solar air flat plate collector for drying application,” *Renew. Sustain. Energy Rev.*, vol. 102, No. 102, pp. 333–345, 2019.

- [27] R. Kumar and M. A. Rosen, "Thermal performance of integrated collector storage solar water heater with corrugated absorber surface," *Appl. Therm. Eng.*, vol. 30, No. 13, pp. 1764–1768, 2010.
- [28] R. H. Martín, J. Pérez-García, A. García, F. J. García-Soto, and E. López-Galiana, "Simulation of an enhanced flat-plate solar liquid collector with wire-coil insert devices," *Solar Energy*, vol. 85, No. 3, pp. 455–469, 2011.
- [29] S. Hossain, A. W. Abbas, J. Selvaraj, F. Ahmed, and N. B. A. Rahim, "Experiment of a Flat Plate Solar Water Heater Collector with Modified Design and Thermal Performance Analysis," *Appl. Mech. Mater.*, vol. 624, pp. 332–338, 2014.
- [30] J. Zhao, Z. P. Wang, K. Z. Wang, and X. Lu, "Analysis of Thermal Performance of Solar Collector in Solar Water Heating System," *Adv. Mater. Res.*, vol. 1055, pp. 193–198, 2014.
- [31] Z. Wang, F. Qiu, W. Yang, and X. Zhao, "Applications of solar water heating system with phase change material," *Renewable and Sustainable Energy Reviews*, vol. 52, pp. 645–652, 2015.
- [32] S. K. Verma, A. K. Tiwari, and D. S. Chauhan, "Performance augmentation in flat plate solar collector using MgO/water nanofluid," *Energy Convers. Manag.*, vol. 124, pp. 607–617, 2016.
- [33] K. Balaji, S. Iniyan, and R. Goic, "Thermal performance of solar water heater using velocity enhancer.pdf." 2017.
- [34] D. G. Gunjo, P. Mahanta, and P. S. Robi, "CFD and experimental investigation of flat plate solar water heating system under steady state condition," *Renewable Energy*, vol. 106, pp. 24–36, 2017.
- [35] L. Anto Joseph Deeyoko, K. Balaji, S. Iniyan, and C. Sharmeela, "Exergy, economics and pumping power analyses of flat plate solar water heater

- using thermal performance enhancer in absorber tube,” *Applied Thermal Engineering*. pp. 726–737, 2019.
- [36] M. R. Assari, H. B. Tabrizi, H. Kavooosi, and M. Moravej, “Design and Performance of Dual-Purpose Solar Collector,” No. August, pp. 1–6, 2007.
- [37] A. V. AK and P. Arun, “Simulation studies on porous medium integrated dual purpose solar collector,” *Int. J. Renew. Energy Res.*, vol. 3, No. 1, pp. 114–120, 2013.
- [38] A. Mohajer, O. Nematollahi, M. M. Joybari, S. A. Hashemi, and M. R. Assari, “Experimental investigation of a Hybrid Solar Drier and Water Heater System,” *Energy Convers. Manag.*, vol. 76, pp. 935–944, 2013.
- [39] R. Venkatesh and W. Christraj, “Experimental Investigation of Multipurpose Solar Heating System,” *J. Energy Eng.*, vol. 141, No. 3, pp. 04014009-1-04014009-10, 2013.
- [40] D. Zhang, J. Li, Z. Gao, L. Wang, and J. Nan, “Thermal performance investigation of modified flat plate solar collector with dual-function,” *Appl. Therm. Eng.*, vol. 108, pp. 1126–1135, 2016.
- [41] T. Rajaseenivasan and K. Srithar, “Potential of a dual purpose solar collector on humidification dehumidification desalination system,” *Desalination*, vol. 404. pp. 35–40, 2017.
- [42] J. Ma *et al.*, “The thermal behavior of a dual-function solar collector integrated with building: An experimental and numerical study on the air heating mode,” *Energies*, vol. 11, No. 9, 2018.
- [43] “COMSOL Multiphysics.” [Online]. Available: <https://www.comsol.com/>.
- [44] B. Wang, B. . Khoo, Z. . Xie, and Z. . Tan, “Fast centroidal Voronoi Delaunay triangulation for unstructured mesh generation,” *J. Comput. Appl. Math.*, vol. 280, pp. 158–173, 2015.

- [45] J. Chen, Y. Huang, D. Wang, and X. Xie, “Adaptive tetrahedral mesh generation by constrained centroidal voronoi-delaunay tessellations for finite element methods,” *Numerical Methods for Partial Differential Equations*, vol. 30, No. 5. pp. 1633–1653, 2014.
- [46] W. Wang and Y. Lu, “Analysis of the Mean Absolute Error (MAE) and the Root Mean Square Error (RMSE) in Assessing Rounding Model,” *Mater. Sci. Eng.*, vol. 324, No. 1, 2018.

APPENDICES

Appendix (A)

The calibration of Instruments used in the experiments

A.1 Calibration of solar collector meter:

Figure (A.1) represents the solar irradiance meter calibration. In the faculty of technical engineering / Najaf, the solar meter is calibrated with the solar energy research station. The data were collected for every thirty minutes between 9:00 AM and 3:00 PM.

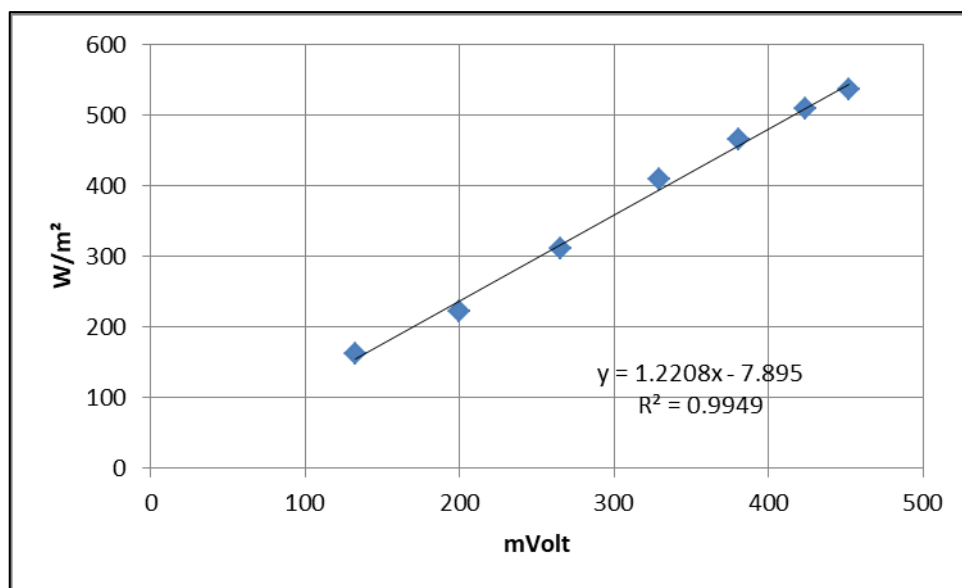


Fig. A.1: Calibration of solar radiation meter.

A.2 Flow rate meter calibrate method

The volumetric rate device is adjusted utilizing cylindrical graduated glass vessels and stopwatch. The section below displays the calibration measures with test results. The calibrator time weight method used to calibrate the volume flow meter with a stopwatch and graduated glass vessel, the calibration is done

by flowing the water through a flow meter at different flow rates and at the same time measuring the flow time required by volume by the pail to fill the correct amount of working fluid.

Samples of volume flow meter calibration

The reading of volumetric flow rate of flow rate meter = 1 liter/min

Inspection no (1):

Monitoring time = for one minute

Water discharge in graduate vessel = 0.97 liter/min.

Inspection no (2):

Monitoring time = for one minute

Water discharge in graduate vessel = 0.966 liter/min.

Inspection no (3):

Monitoring time = for one minute

Water discharge in graduate vessel = 0.954 liter/minute

Inspection no (4):

Monitoring time = for one minute

Water discharge in graduate vessel = 0.994 liter/minute.

The average of volumetric flow rates

$V = (v_1 + v_2 + v_3 + v_4) / 4 = (0.994 + 0.954 + 0.966 + 0.97) / 4 = 0.971$ liter/minute the error of the volume flow meter = $1 - 0.971 = 0.029$ liter/minute

$$\% \text{ Error} = \frac{1 - 0.029}{1} \times 100 = 2.9\%$$

A.3 Calibration of temperature sensors of 8- channel data logger and 4K type thermocouples with digital thermometers:

The two sets of sensors (S1 – S8) °C, (S9-S16) °C for two 8- channel data loggers and four thermocouples (T1-T4) °C for digital thermometer are calibrated by using a mercury thermometer. The calibration results were recorded in the tables (A-1), (A-2) and (A-3).

Table A.1: Calibration results of first 8- channels data logger with 8 sensors.

Mercury Thermometer °c	S 1°c deeg.	S 2°c deeg	S 3°c deeg	S 4°c deeg	S 5°c deeg	S 6°c deeg	S 7°c deeg	S 8°c deeg
20	20.4	20.4	20.3	19.8	19.7	20.3	20.4	19.6
25	25.5	25.4	24.6	24.7	25.4	25.3	25.4	24.7
30	30.4	30.3	30.5	29.7	30.4	30.3	30.4	29.6
35	35.4	35.4	35.3	35.4	34.6	35.4	35.2	34.7
40	40.3	40.2	40.2	40.2	39.9	39.8	40.2	40.3
45	45.2	45.4	44.7	44.6	45.2	45.2	45.3	44.9
50	50.3	50.4	49.6	49.7	50.1	50	50.3	50.2
55	55.4	55.3	54.6	55.1	55.3	54.6	55.2	55.3
60	60.3	60.4	60.3	60.1	59.7	60.2	60.2	60.2
65	64.5	65.4	64.5	64.5	65.5	64.6	64.8	64.6

Table A.2: Calibration results of second 8- channels data logger with 8 sensors.

Mercury Thermometer deeg	S 9 °C deeg.	S 10 °C deeg.	S 11 °C deeg.	S 12 °C deeg.	S 13 °C deeg.	S 14 °C deeg.	S 15 °C deeg.	S16 °C deeg.
20	20.4	19.4	20.4	19.8	20.4	19.7	20.3	19.8
25	24.8	25.4	25.4	25.3	25.4	24.7	25.3	25.3
30	30.4	30.5	30.3	29.7	30.3	29.8	29.6	30.4
35	35.5	35.3	35	34.6	35.3	34.7	34.9	34.7
40	40.4	40.3	40	39.7	39.6	40.4	39.8	39.8
45	45.4	45	44.7	44.6	45.4	44.8	45.4	45.3
50	50.3	50	50.4	49.6	49.8	50.1	50.3	50.2
55	55.3	55.2	55	54.6	54.7	55.4	55.3	54.6
60	60.4	60.3	60	60.4	59.7	59.8	60	60.4
65	64.3	65	64.7	64.7	64.8	64.5	65	64.4

Table A.3: The calibration of 4 k- type thermocouple.

Mercury Thermometer °C	Temp1 °C	Temp.2 °C	Temp.3 °C	Temp.4 °C
25	25.9	26	26	26
30	31	29.2	31	31
35	36	35.6	36	36.3
40	41	40.9	41	41
45	44.1	46	46	46
50	49.2	51	51	51
55	54.1	54	56	56
60	60	61	61.2	59
65	64	64	64.1	66

The values of sixteen temperature sensors for two 8- channel data loggers and four thermocouples are too close that they cannot be distinguished if plotted. Correlating the values above (straight lines) calibration curves.

a. The correlation values of the first set sensors (S_1 to S_8) as follows:

$$Ts_1=0.988 \times Ts_1 \text{ (real)} + 0.78 \quad \dots\dots\dots \text{(A.1)}$$

$$Ts_2=0.99 \times Ts_1 \text{ (real)} + 0.3752 \quad \dots\dots\dots \text{(A.2)}$$

$$Ts_3=0.9886 \times Ts_3 \text{ (real)} + 0.4442 \quad \dots\dots \text{.(A.3)}$$

$$Ts_4=0.9993 \times Ts_4 \text{ (real)} - 0.0841 \quad \dots\dots\dots \text{(A.4)}$$

$$Ts_5=1.0035 \times Ts_5 \text{ (real)} - 0.0794 \quad \dots\dots\dots \text{.(A.5)}$$

$$Ts_6=0.9851 \times Ts_5 \text{ (real)} + 0.6836 \quad \dots\dots\dots \text{(A.6)}$$

$$Ts_7=0.991 \times Ts_7 \text{ (real)} + 0.6212 \quad \dots\dots\dots \text{.(A.7)}$$

$$Ts_8=1.0064 \times Ts_8 \text{ (real)} - 0.263 \quad \dots\dots\dots \text{.(A.8)}$$

Where: $Ts \text{ (real)}$ = measured values; $Ts_1 \dots s_8$ = correction values.

b. The correlation values of the second set sensors (S_9 to S_{16}) as follows:

$$T_{S_9} = 0.9918 \times T_{S_9} (\text{real}) + 0.5703 \quad \dots\dots (A.9)$$

$$T_{S_{10}} = 1.0024 \times T_{S_{10}} (\text{real}) + 0.37 \quad \dots\dots\dots (A.10)$$

$$T_{S_{11}} = 0.9882 \times T_{S_{11}} (\text{real}) + 0.5897 \quad \dots\dots\dots (A.11)$$

$$T_{S_{12}} = 0.999 \times T_{S_{12}} (\text{real}) - 0.1588 \quad \dots\dots\dots (A.12)$$

$$T_{S_{13}} = 0.983 \times T_{S_{13}} (\text{real}) + 0.7612 \quad \dots\dots\dots (A.13)$$

$$T_{S_{14}} = 0.003 \times T_{S_{14}} (\text{real}) - 0.2388 \quad \dots\dots\dots (A.14)$$

$$T_{S_{15}} = 1.0006 \times T_{S_{15}} (\text{real}) + 0.0642 \quad \dots\dots\dots (A.15)$$

$$T_{S_{16}} = 0.9941 \times T_{S_{16}} (\text{real}) + 0.2424 \quad \dots\dots\dots (A.16)$$

c. The correlation values of thermocouples (T_1 to T_4) as follows:

$$T_1 = 0.946 \times T_1 (\text{real}) + 2.4633 \quad \dots\dots\dots (A.17)$$

$$T_2 = 0.978 \times T_2 (\text{real}) + 1.8011 \quad \dots\dots\dots (A.18)$$

$$T_3 = 0.9767 \times T_3 (\text{real}) + 1.8611 \quad \dots\dots\dots (A.19)$$

$$T_4 = 0.981 \times T_4 (\text{real}) + 1.155 \quad \dots\dots\dots (A.20)$$

Appendix (B)

The experimental results

Table B-1 showing the sample of experimental results for one day at 18/6/2020

Table B-1 Experimental results.

Time	Ta_out (°C)	Tw_out (°C)	Qu_a (W)	Qu_w (W)	η (%)
8:00	47.6	44.8	131.5	596.7	58.6
9:00	60.2	47.9	156.3	685.9	56.6
10:00	65.4	52	584.6	767.7	64.5
11:00	71.1	56.5	441.8	752.9	74.7
12:00	75.1	60.3	493.1	767.7	73.2
13:00	76.1	64.5	479.1	730.5	58.9
14:00	73.8	66.8	448.1	474	49.6
15:00	70.3	65.5	285.3	329	46.3
16:00	62.4	61.1	148	61.3	40.3
17:00	52.9	59.8	80.9	0	29.2
18:00	48.2	55.1	11.3	0	21.7

Appendix (C)

Uncertainties analysis

In the present analysis, some of the sources of error which could be defined as sources of uncertainty in estimating volumetric flow rates, temperatures and drops in pressure and solar radiation which could lead to errors in the predicted values.

C.1 collector efficiency derivation

Collector efficiency is calculated from the ratio of output heat to input heat for solar collector.

$$\eta = \left(\frac{Q_{out}}{Q_{in}} \right), \quad \eta = \frac{\left(\frac{\Delta Q}{Q} \right)_{out}}{\left(\frac{\Delta Q}{Q} \right)_{in}}$$

Where the Q_{out} represents the heat gained by the water from the inlet to outlet. Thus Q_{out} is given by:

$$Q_{out} = \dot{m} \times C_p \times (T_o - T_i)$$

$$\left(\frac{\Delta Q}{Q} \right)_{out} = \left(\frac{1}{Q_{out}} \right) \left[\left\{ \frac{\partial Q_{out}}{\partial \dot{m}} \Delta \dot{m} \right\}^2 + \left\{ \frac{\partial Q_{out}}{\partial T_o} \Delta T_o \right\}^2 + \left\{ \frac{\partial Q_{out}}{\partial T_i} \Delta T_i \right\}^2 \right]^{0.5}$$

$$\left(\frac{\Delta Q}{Q} \right)_{out} = \left[\left\{ \frac{\Delta \dot{m}}{\dot{m}} \right\}^2 + \left\{ \frac{\Delta T_o}{T_o} \right\}^2 + \left\{ \frac{\Delta T_i}{T_i} \right\}^2 \right]^{0.5} \quad (C/1)$$

Q_{in} Is the input heat evaluated from atmospheric temperature and inlet temperature of water:

$$\left(\frac{\Delta Q}{Q} \right)_{in} = \frac{1}{Q_{in}} \left[\left\{ \frac{\partial Q_{in}}{\partial T_i} \Delta T_i \right\}^2 + \left\{ \frac{\partial Q_{in}}{\partial T_a} \Delta T_a \right\}^2 + \left\{ \frac{\partial Q_{in}}{\partial G_T} \Delta G_T \right\}^2 \right]^{0.5}$$

$$\left(\frac{\Delta Q}{Q}\right)_{in} = \left[\left\{ \frac{\Delta T_i}{T_i} \right\}^2 + \left\{ \frac{\Delta T_a}{T_a} \right\}^2 + \left\{ \frac{\Delta G_T}{G_T} \right\}^2 \right]^{0.5} \quad (C/2)$$

$$\frac{\Delta \eta}{\eta} = \frac{1}{\eta} \left[\left\{ \frac{\partial \eta}{\partial Q_{in}} \Delta Q_{in} \right\}^2 + \left\{ \frac{\partial \eta}{\partial Q_{out}} \Delta Q_{out} \right\}^2 \right]^{0.5}$$

$$\frac{\Delta \eta}{\eta} = \left[\left\{ \frac{\Delta Q_{in}}{Q_{in}} \right\}^2 + \left\{ \frac{\Delta Q_{out}}{Q_{out}} \right\}^2 \right]^{0.5} \quad (C/3)$$

Appendix (D)

List of publications

- 1- Published of the paper “**Simulation analysis of thermal performance of the solar air/water collector by using computational fluid dynamics**” by E3S Web of Conferences (TE-RE-RD 2020).

E3S Web of Conferences **180**, 02015 (2020)
 TE-RE-RD 2020

<https://doi.org/10.1051/e3sconf/202018002015>

Simulation analysis of thermal performance of the solar air/water collector by using computational fluid dynamics

*Jafer Shandal*¹, *Qahlan A Abed*^{2*}, and *Dhafer M. Al-Shamkhee*³

^{1,2}Engineering technical college/ Najaf, Al - Furat Al- Awsat Technical University, 31001, Iraq

³Technical Institute/ Al-Rumaitha, Al - Furat Al- Awsat Technical University, 31001, Iraq

Abstract. Utilizing solar energy has received a giant activity by energy applications into distinctive states within the world. The sun is regarded strong supply providing uninterrupted coherent energy. In this research, simulation study has been done to estimate the performance of dual purpose solar collector (DPSC). Flat plate dual purpose solar collector with dimensions (194 cm length, 95 cm width and 14 cm thickness) has been used for heating the air and water for different using. Rectangular fins are used in air duct to increase heat transfer coefficient in air heater part. COMSOL Multiphysics 5.4 computer program has been used to calculate the theoretical results. Many parameters such as a different flow rate and temperatures for the inlet working fluids are investigated.

1 Introduction

One of the most serious matters in the world is energy. As we know, there are many sources to get the energy. The most important of which is the most common fossil fuel, but, because of the many problem caused by fossil fuel, the attention have been given to searchers for another sores. Solar energy is considered more renewable energy using thermal collectors. These collectors are most common type of solar energy applications. Assari et al [1] Studied an experimental and theoretical investigation performance of two working fluid solar collector to product hot air and hot water. To improve the performance of the hybrid air and water collector, the authors used various air forms of air ducts. They showed that the rectangular fin types have better performance. Nematollahi et al [2] Published an experimental study to investigate the two different types of flat solar collector's effectiveness. Using dual purpose solar collector (DPSC) decreases costs and required space. Venkatesh and Christraj [3] Carry out an experimental study on same collector which design by M.R. Assari et al. But in this study, the authors studied dray a mixture of three vegetable types; dill the first one, parsley second and the last one was coriander at constant air and water flow rates. The obtained results were evaluated with other results had been obtained from the solar drier collector have an electrical heater. The results appear that the dryer solar collector with an electrical heater has 20 °C -30 °C

- 2- Published the paper “**A review on development of solar thermal flat plate collector**” by IOP Conference Series: Materials Science and Engineering.

2nd International Scientific Conference of Al-Ayen University (ISCAU-2020) IOP Publishing
 IOP Conf. Series: Materials Science and Engineering 928 (2020) 022051 doi:10.1088/1757-899X/928/2/022051

A review on development of solar thermal flat plate collector

Jafer Shandal¹ and Qahtan A. Abed^{2,1}

¹ Engineering technical college/ Najaf, Al - Purat Al- Awsat Technical University, Iraq


² Technical Institute/ Al-Rumaiha, Al - Purat Al- Awsat Technical University, Iraq
qrasaiafer@gmail.com

Abstract

Solar thermal collectors are most frequent type of solar energy applications. Solar collector is a type of heat exchanger where heat exchanges take place between a distance source and a moving heat transfer fluid in the collector. Solar collectors can be categorized as concentrated and non-concentrating according to their design. In this present work, the most important studies that dealt with the development in the manufacture of collectors were reviewed. Studies differed according to the type of improvement discussed, such as use of obstacles, type of fin, absorber plate design, nanofluid as heat transfer fluid and use of enhancement devices. Researchers can take advantage of simulation programs to get the best experiences at the lowest cost and time.

1 Introduction

One of the most serious matters in the world, is Energy. As we know, there are multiple sources of energy. The most important of which is the most common Fossil fuel, but, because of the many problem caused by fossil fuel, the attention

 Content from this work may be used under the terms of the [Creative Commons Attribution 3.0 license](https://creativecommons.org/licenses/by/3.0/). Any further distribution of this work must maintain attribution to the author(s) and the title of the work, journal citation and DOI.
 Published under license by IOP Publishing Ltd 1

الخلاصة

تم في هذا البحث دراسة أداء المجمع الحراري الشمسي ثنائي الغرض تجريبياً وعدادياً. تضمنت الدراسة دراسة تصميم نوع جديد للوح الامتصاص وتوزيع أنابيب الماء. تم إجراء جزء المحاكاة من هذا البحث باستخدام برنامج (COMSOL Multiphysics) كان التصميم الجديد عبارة عن لوح امتصاص متعرج بأبعاد (٢ * ١) م وأنابيب ماء متعرجة بقطر (٠,٠١) م تمر عبر لوح الامتصاص.

تم إجراء العمل التجريبي في مدينة المثنى في العراق على خط عرض ٣١ ° ٢٦ ' ٢٩,٤٥٦١" شمالاً وخط طول ٤٥ درجة ٢٦ ' ٥٠,٦٧١٤" هـ. تم دراسة تأثير كل من الإشعاع الشمسي ودرجة الحرارة المحيطة وسرعة الرياح وتدفق المياه الحجمي ودرجة حرارة الماء الداخل على أداء المجمع الحراري الشمسي ثنائي الغرض. أظهرت نتائج المحاكاة العددية أن العمل الحالي حقق تعزيزاً في كفاءة المجمع بنسبة ٢,٤٪ مقارنة بالدراسة السابقة ، وأيضاً وجد أنه عندما يزيد الإشعاع الشمسي ودرجة حرارة الماء الداخل ودرجة الحرارة المحيطة تزداد درجة الحرارة الخارجة ، ولكنها تقل مع سرعة الرياح وزيادة التدفق الحجمي. يوجد توافق جيد بين المحاكاة العددية والنتائج التجريبية بمتوسط خطأ حوالي ٤,٧٢٪.

تضمن العمل التجريبي دراسة تأثير ثلاث نطاقات من التدفق الحجمي (٤٠ ، ٦٠ ، ٨٠ لتر / ساعة في شهري يونيو ويوليو لسنة ٢٠٢٠). وأظهرت النتائج التجريبية أن المعدل الأمثل للجريان الحجمي هو ٤٠ لتر / ساعة. وبلغت أعلى درجة حرارة خروج الماء والهواء (٦٩,٩ و ٧٩,٢) درجة مئوية على التوالي. كانت أعلى قيم الكفاءة المسجلة (٨٣,٣ ، ٨٠,٤ ، ٧٨,٥)٪ لـ (٤٠ ، ٦٠ ، ٨٠) لتر / ساعة على التوالي.



جمهورية العراق

وزارة التعليم العالي والبحث العلمي

جامعة الفرات الاوسط التقنية

الكلية التقنية الهندسية - نجف

محاكاة تجريبية وعددية لمجمع حراري شمسي ثنائي الغرض

رسالة مقدمة الى

قسم تقنيات ميكانيك القوى

كجزء من متطلبات نيل درجة الماجستير تقني في هندسة الميكانيكية (حراريات)

تقدم بها الطالب

جعفر شندل مطر

(بكالوريوس هندسة تقنيات السيارات ٢٠١٣)

اشراف

الأستاذ المساعد الدكتور قحطان عدنان عبد

محرم ١٤٤٢ هـ